10.24425/acs.2021.138692

Archives of Control Sciences
Volume 31(LXVII), 2021
No. 3, *pages 553–591*

Power system oscillation damping controller design: a novel approach of integrated HHO-PSO algorithm

Ramesh DEVARAPALLI and Vikash KUMAR

The hybridization of a recently suggested Harris hawk's optimizer (HHO) with the traditional particle swarm optimization (PSO) has been proposed in this paper. The velocity function update in each iteration of the PSO technique has been adopted to avoid being trapped into local search space with HHO. The performance of the proposed Integrated HHO-PSO (IHHOPSO) is evaluated using 23 benchmark functions and compared with the novel algorithms and hybrid versions of the neighbouring standard algorithms. Statistical analysis with the proposed algorithm is presented, and the effectiveness is shown in the comparison of grey wolf optimization (GWO), Harris hawks optimizer (HHO), barnacles matting optimization (BMO) and hybrid GWO-PSO algorithms. The comparison in convergence characters with the considered set of optimization methods also presented along with the boxplot. The proposed algorithm is further validated via an emerging engineering case study of controller parameter tuning of power system stability enhancement problem. The considered case study tunes the parameters of STATCOM and power system stabilizers (PSS) connected in a sample power network with the proposed IHHOPSO algorithm. A multi-objective function has been considered and different operating conditions has been investigated in this papers which recommends proposed algorithm in an effective damping of power network oscillations.

Key words: Harris hawk optimization, Power system stabilizers, STATCOM, FACTS, particle swarm optimization

1. Introduction

1.1. Motivation and research background

The process of optimization involves the search for the best possible solution for a specific problem with certain constraints. These optimization problems can be the real-world problem from the field of engineering, economics, business, pattern recognition, control objectives, image processing, filter modelling etc., that

Ramesh Devarapalli (corresponding author, e-mail: ramesh.ee@bitsindri.ac.in) and Vikash Kumar (e-mail: kr.vikash104@gmail.com are with Department of Electrical Engineering, B.I.T. Sindri, Dhanbad, Jharkhand, India.

Received 18.01.2021. Revised 26.07.2021.

do not have any proper accurate solution [1]. Modern metaheuristic algorithms are capable of dealing with robust optimization as it offers good computation power, and they do not require substantial computation time. Some of the algorithms with their inspiration of design has been listed in Table 1. Most of the proposed algorithms needs to address the following two main issues, i.e. No free lunch theorem (NFL) and determination of exploration and exploitation process. The NFL theorem suggests logically that a particular algorithm cannot be suited for solving all the optimization problem [2]. This means that a specific algorithm may be best suited for a given set of problems but can fail for other problem sets. The other issue of an algorithm is that it must have a balanced exploration and exploitation process. It is evident that too much exploitation leads to a trapped local optimum, whereas excess exploration leads to unsuitable results hence proper balance between the two is necessary [3].

Table 1: Few optimization algorithms and their inspiration

Algorithm	Inspiration	Year
Simulated Annealing (SA) [7]	Metallurgical annealing	1983
Genetic Algorithm (GA) [8]	Evolution	1975
Particle Swarm Optimization (PSO) [9]	Bird flock	1995
Artificial fish-swarm Algorithm (AFSA) [10]	Fish and Bird flock	2003
Ant Colony Optimization (ACO) [11]	Ant colony	1996
Termite Algorithm (TM) [12]	Termite colony	2006
Artificial Bee Colony (ABC) [13]	Honey bee	2006
Wasp Swarm Algorithm (WSA)	Movement of Wasps in nature	2007
Monkey Search (MS) [14]	Monkey climbing process	2007
Imperialistic Competitive Algorithm (ICA) [15]	Imperialistic competition	2007
Biogeography Based Optimizer (BBO) [16]	Study of biological organisms in terms of geographical distribution	2008
Firefly Algorithm (FA) [17]	Social behavior of fireflies	2009
Group Search Optimizer (GSO) [18]	Animal searching behavior	2009
Gravitational Search Algorithm (GSA) [19]	Law of gravity	2009
Fireworks Algorithm (FA) [20]	Explosion behavior of firework	2010
Bat Algorithm (BA) [21]	Echo location behavior of bat	2010
Fruit Fly Optimization (FFO) [22]	Fruit foraging behavior	2012
Flower Pollination Algorithm (FPA) [23]	Pollination process of flowering species	2012
Krill Herd (KH) [24]	Herding behavior of Krill	2012
Dolphin Echolocation (DE) [25]	Echolocation ability of Dolphin	2013

Table 1 [cont.]

Algorithm	Inspiration	Year
Grey Wolf Optimization (GWO) [26]	Hunting behavior of grey wolves	2013
Black Hole Optimization (BHO) [27]	Black Hole phenomena	2013
Mine Blast Algorithm (MBA) [28]	Mine bomb explosion	2013
Dragonfly Algorithm (DA) [29]	Swarming behavior of dragonflies	2015
Moth Flame Optimization (MFO) [30]	Movement of Moths around a light source	2015
Henry Gas Solubility Optimization (HGO) [31]	Governed by Henry's gas law	2015
Ant Lion Optimizer (ALO) [32]	Hunting nature of ant lion	2015
Lightening Search Algorithm (LSA) [33]	Natural phenomena of lightening	2015
Artificial Algae Algorithm (AAA) [34]	Living behavior of microalgae	2015
Virus Colony Search (VCS) [35]	Virus infection and diffusion	2016
Shark Smell Optimization (SSO) [36]	Ability of shark in finding its prey by smell sense	2016
Multi-Verse Optimizer (MVO) [37]	Multiverse theory	2016
Whale Optimization Algorithm (WOA) [38]	Social behavior of humpback whale	2016
Crow Search Algorithm (CSA) [39]	Intelligent food hiding behavior of crows	2016
Dolphin Swarm Optimization Algorithm (DSOA) [40]	Mechanisms of dolphin in detecting, chasing and preying on swarms of sardines	2016
Sine Cosine Algorithm (SCA) [41]	Fluctuating behavior of sine and cosine function	2016
Thermal Exchange Optimization (TEO) [42]	Newtons law of cooling	2017
Grasshopper Optimization Algorithm (GOA) [43]	Swarming behavior of grasshopper	2017
Electro Search Algorithm (ESA) [44]	Orbital movement of electrons around the nucleus	2017
Spotted Hyena Optimizer (SHO) [45]	Social behavior of spotted hyena	2017
Human Behavior-Based Optimization (HBBO) [46]	Human behavior is the main source of inspiration	2017
Lightening Attachment Procedure Optimization (LAPO) [47]	Lightening attachment process	2017
Salp Swarm Algorithm (SSA) [48]	Swarming behavior of Salp during navigating and foraging in oceans	2017
Mouth Brooding Fish Algorithm (MBFA) [49]	Lifecycle of mouth brooding fish	2017
Butterfly-Inspired Algorithm (BIA) [50]	Mate searching mechanism of butterfly	2017

1.2. Literature review

The recent development in computational intelligence has opened a gateway to a number of nature-inspired optimization algorithm which imitates the natural or biological behaviour of the organisms in the environment [4]. In the literature, nature-inspired algorithms are basically classified under the categories of the evolutionary algorithm [5], swarm intelligence and physics-based algorithm [4]. The evolutionary algorithms are based on the evolutionary process of a natural organism [6]. It randomly generates a set of a possible solution and runs a number of iterations with self-improvement of the best-fitted solution. Evolutionary algorithms are often known as genetic algorithms. They are relatively slow at approaching the best possible solution. The main concept is based on the Darwin's theory of evolution i.e. evolutionary process is slow as it consists of a series of small steps starting from a bad position and moving through moderate state it reaches to the best state. All the evolutionary algorithms follow a similar pattern where a population of individuals is in an environment with a limited amount of resources. Under this competitive condition natural selection process begins (i.e. survival of the fittest). Two important ideas that forms the basis of evolutionary systems are: (i) Recombination and mutation to create diversity in the population, thereby promoting novelty. (ii) Selection scheme that brings the mean quality of solutions in the population after each mutation. Genetic Algorithms do not need any gradient information of solutions as it evaluates the individuals based on fitness and hence are suitable for such real-life problems with unknown search space.

In the case of swarm intelligence algorithm, they utilize the information of the search space to proceed with the algorithm. Some of the recent optimizing algorithm based on this concept are PSO, CS, DA, GWO, ACO, MFO ADC, etc. All Swarm intelligence-based algorithms use some of the natural behaviour of herds or group of animals encoded in their algorithms where the heard acts a population or search agent to reach to a best possible solution in the specified range Similarly, the moth flame algorithm is inspired by the movement tendency of moths in a full moon night or around a particular light source [51]. Seyedali Mirjalili and Andrew first proposed grey wolf optimization in 2013. The fundamental idea behind the algorithm is based on the hunting technique and social hierarchy of grey wolves in their pack. GWO gives exceptional results for unimodal functions. They have been successfully implemented on the real engineering problems such as aligning multiple molecular sequences, Maximum power point tracking of the PV system, Design of plug type triggers for composite square tubes etc. Ant system: Optimization by colony of cooperating ants, proposed by Dorigo and Colorni in 1996 is inspired by food searching behaviour of some species of ant. These ants produce a particular pheromone which helps them to mark some favourite spots on the ground and on the path, which is followed by all the members of the colony [52].

Almost all physics-based algorithms are inspired by the physical laws of the universe, such as GSA, MVO, CSS etc. Gravitational Search Algorithm (GSA) is based on the law of gravity which states that "Every particle in the universe attracts every other particle with a force which is directly proportional to the product of their masses and inversely proportional to the square of their distance". Here the search agents are objects (collection of masses), and their mean of masses are considered as the performance index [19]. Another physics-based optimization algorithm is Multi-Verse Optimization (MVO). It is based on the concept of cosmology (white hole, black hole and wormhole). Here it is believed that Big Bang creates a new universe. Similarly, multiple big bangs create multiple universes. These universes can intersect, collide and interact with each other. The concept of white hole and black hole is utilized for exploring search space, and the concept of wormholes is used exploiting the search space and solutions are the objects of the universe [37].

Metaheuristics are inspired by simple concepts of nature and hence this simplicity allows us to hybridize two or more metaheuristics to improve the computational ability of the existing ones. The modification usually includes improvements in certain parameters of the algorithm by merging together, two or more individual algorithm such as HSO-PSO, GWO-PSO etc. Any two or more algorithms are combined to form a hybrid in a high-level or low-level or co-evolutionary form as homogeneous or heterogeneous. For instance, PSO-GSA [53](Particle Swarm Optimization Gravitational Search Algorithm) is a combination of PSO [9] and GSA [19]. These two algorithms are hybridized to combine their individual advantages into one. The exploration ability of PSO is merged with the local search ability (exploration) of GSA to get the best possible outcome. Another good example of a hybrid algorithm is PSO-GWO [54].

1.3. Contribution

Based on the literature, the main contribution of the paper is to suggest an integrated HHO-PSO (IHHO-PSO) algorithm to improve the capability of HHO algorithm in solving the complex optimization problems with the aid of well-known PSO algorithm. HHO is a population-based gradient-free optimization algorithm. It mimics the cooperative behaviour and hunting style of Harris hawk. HHO is usually implemented in designing problems of industrial goods such as Three bar truss design, Pressure vessel design, Welded beam design, Multi-plate disc clutch brake, rolling element bearing design [55], parameter identification of photovoltaic cells [56] etc. Eberhart and Kennedy proposed Particle Swarm Optimization in 1995 for the optimization of continuous non-linear functions. The movement of organisms inspires it in a group or swarms; however, the algorithm was initially built on the bird flocking tendency or fish flocking [9]. PSO has a convincing exploitation ability but poor exploration ability (required for a good starting position), on the other hand HHO algorithm has a high exploration ability hence it gives a good starting point. Therefore, these two unique features of both the algorithm are fused together to obtain a hybrid HHO-PSO.

1.4. Paper organization

The proposed algorithm has been demonstrated on the benchmark mathematical functions using statistical analysis. A real-time electrical power system stability enhancement problem has been considered and solved the optimal controller parameter selection using the proposed algorithm. The whole work is organized as follows: Section 2 demonstrates the proposed algorithm and is realized on the benchmark functions in Section 3. Section 4 gives the case study design, and Section 5 investigates the performance characteristics obtained from the proposed controller on it. The conclusions, references and other system parameters have been listed in the end.

2. IHHO-PSO algorithm

2.1. HHO overview

Ali Asghar Heidari, Seyedali Mirijalili and his team proposed Harris hawk's optimization in 2018 which is mainly used to solve single objective optimization problems efficiently. HHO is basically a gradient-free population-based optimization algorithm. The central idea of HHO is based on the cooperative hunting behaviour of Harris hawk bird, especially their chasing style of prey which is called surprise pounce or also known as 'seven kill' strategy. Their hunting pattern also dynamic in nature and changes based on the physical scenario and the type of the prey. This intelligent cooperative behaviour of Harris hawk while hunting is mimicked mathematically to develop the optimization algorithm. These activities are mathematically modelled as exploring the prey, exploitation, and transition from exploration to exploitation as follows.

Exploration phase

The exploration of the prey by Harris's hawk can be modelled by considering that the hawks will wait for the prey at different locations to detect the prey as there is possibility that the prey may not be visible instantly. Here Harris hawk are the candidate solution and the best solution is the intended prey. The initial position of an individual hawk depends either arbitrary or based on the other hawks in their group as given in (1).

$$X(iter{+}1) = \begin{cases} X_{\text{arb}}(iter) - r_1 \left| X_{\text{arb}}(iter) - 2r_2 X(iter) \right| & q \geqslant 0.5, \\ \left(X_{\text{prey}}(iter) - X_m(iter) \right) - r_3 \left(\text{LB} + r_4(\text{UB} - \text{LB}) \right) & q < 0.5, \end{cases} \tag{1}$$

where $X(iter)$ position vector of a hawk for the iteration '$iter$' with arbitrary values of r_1, r_2, r_3, r_4 and q within (0, 1). UB and LB are the upper and the lower bounds of the randomly selected Harris hawk. The average hawk position X_m obtained for N number of hawks can be expressed as,

$$X_m(iter) = \frac{1}{N} \sum_{i=1}^{N} X_i(iter). \tag{2}$$

As the exploration phase of hawks made based on different trails, they will identify the prey. As the energy of the prey is being lowered in the process of escaping, hawks will move to the exploitation phase. This transition can be mathematically modelled as in (3). The escaping energy of the prey with an initial energy of E_0 can be modelled as

$$E = 2E_0 \left(1 - \frac{iter}{\text{Max\_}iter}\right). \tag{3}$$

Exploitation Phase:

Based on this phase, Harris' hawks execute the surprise attack or seven murders known as to attack the desired prey perceived at the earlier phase. Therefore, it often tries to escape as hazardous situations. Assume r is the opportunity for prey to escape successfully ($r < 0.5$) or not to escape successfully ($r \geqslant 0.5$) prior to the attack of surprise. This reward, $|E| \geqslant 0.5$, a mild siege occurs, as well as $|E| < 0.5$, hard besiege happens.

The escaping energy with $E \geqslant 0.5$ is defined as soft besiege and $E < 0.5$ is defined as hard besiege. The position update for the cases are given as,

$$X(iter+1) = \begin{cases} \Delta X(iter) - E|J\,X_{\text{prey}}(iter) - X(iter)| & |E| \geqslant 0.5, \\ X_{\text{prey}}(iter) - E|\Delta X(iter)| & |E| < 0.5, \end{cases} \tag{4}$$

$$\Delta X(iter) = X_{\text{prey}}(iter) - X, \tag{5}$$

where, $J = 2(1 - r_5)$ with random value of r_5 in (0,, 1).

The exploitation phase is further improved in obtaining the optimal solution based on the opportunity 'r' factor. It further utilizes the levy random walk function for the soft/hard besiege, which is explained in detail in [57]. Hence, HHO has a proper balance between the exploratory and exploitative tendencies on the problem with multiple variables. As it offers a variety of chasing and escaping pattern, such a dynamic pattern is quite helpful in solving a complex engineering problem.

2.2. IHHO-PSO overview

However, there is a possibility of being stuck in local optima that can be resolved by introducing a swarm-based approach to the HHO algorithm. In this research, an integrated HHO-PSO strategy is used to stay away from the weakness that happened by the individual utilization of the strategy. The position update of the hawks in each iteration can be upgraded by using (6), (7).

$$X_{\text{new}}(iter+1) = X(iter) + Vel(iter+1), \tag{6}$$

$$Vel(iter+1) = w \cdot Vel(iter) + C_1 \cdot r_6 \cdot (X(iter) - X_{new}(iter)), \tag{7}$$

where Vel represents the velocity vector, w is the inertia weight parameter, C_1 is the optimization parameter and r_6 is a random value in [0, 1].

3. Realization of IHHO-PSO on benchmark functions

The proposed IHHO-PSO algorithm is tested on the 23-benchmark systems as considered by many researchers [58]. These functions are given in Table 2, Table 3, and Table 4. Unimodal functions have unique global optima, so it serves as a validating mechanism for the exploitation and convergence ability of the

Table 2: Unimodal benchmark functions

Function	Formulation	Dim, limits
Sphere	$f_2(x) = \sum_{i=1}^{n} x_i^2$	30, [–100, 100]
Schwefel 2.22	$f_2(x) = \sum_{i=1}^{n} \lvert x_i\rvert + \prod_{i=1}^{n} \lvert x_i\rvert$	30, [–10, 10]
Schwefel 1.2	$f_3(x) = \sum_{i=1}^{n} \left(\sum_{j=1}^{i} x_j\right)^2$	30, [–100, 100]
Schwefel 2.21	$f_4(x) = \max_i \{\lvert x_i\rvert,\ 1 \leqslant i \leqslant n\}$	30, [–100, 100]
Rosenbrock	$f_5(x) = \sum_{i=1}^{n-1} \left[100\,(x_{i+1} - x_i)^2 + (x_i - 1)^2\right]$	30, [–30, 30]
Step	$f_6(x) = \sum_{i=1}^{n} [x_i + 0.5]^2$	30, [–100, 100]
Quartic	$f_7(x) = \sum_{i=1}^{n} i x_i^4 + random\,(0, 1)$	30, [–1.28, 1.28]

algorithm [59]. Now, the multimodal functions are usually known to have a number of local optimum values [60]. So, it is expected that the algorithm must avoid the local optima to give a suitable global optimum value [4]. Hence these set of benchmark functions serves as a testing mechanism for the exploration capability of the proposed algorithm. Here 'Dim' represents the dimension of the given function, and 'limits' represents the upper and lower boundary of the given function. In the paper, we have used other well-known novel and nature-inspired optimization algorithms such as GWO, HHO, BMO and GWOPSO to compare the computational ability of our proposed integrated HHO-PSO algorithm.

Table 3: Multimodal benchmark functions

Function	Formulation	Dim, limits
Schwefel	$f_8(x) = \sum_{i=1}^{n} -x_i \sin\left(\sqrt{\lvert x_i \rvert}\right)$	30, [–500, 500]
Rastrigin	$f_9(x) = \sum_{i=1}^{n} \left[x_i^2 - 10\cos(2\Pi x_i) + 10\right]$	30, [–5.12, 5.12]
Ackley	$f_{10}(x) = -20\exp\left(-0.2\sqrt{\frac{1}{n}\sum_{i=1}^{n} x_i^2}\right) - \exp\left(\frac{1}{n}\sum_{i=1}^{n}\cos(2\Pi x_i)\right) + 20 + e$	30, [–32, 32]
Griewank	$f_{11}(x) = \frac{1}{4000}\sum_{i=1}^{n} x_i^2 - \prod_{i=1}^{n}\cos\left(\frac{x_i}{\sqrt{i}}\right) + 1$	30, [–600, 600]
Penalized	$f_{12}(x) = \frac{\Pi}{n}\left\{101\sin(\Pi y_1) + \sum_{i=1}^{n-1}(y_i - 1)^2\left[1 + 10\sin^2(\Pi y_{i+1}) + (y_n - 1)^2\right]\right\} + \sum_{i=1}^{n} u(x_i, 10, 100, 4)$ where $y_i = 1 + \frac{x_i + 1}{4}$ and $u(x_i, a, k, m) = \begin{cases} k(x_i - a)^m & x_i > a \\ 0 & -a < x_i < a \\ k(-x_i - a)^m & x_i < -a \end{cases}$	30, [–50,50]
Penalize 2	$f_{13}(x) = 0.1\left\{\sin^2(3\Pi x_1) + \sum_{i=1}^{n} \begin{matrix} (x_i - 1)^2\left[1 + \sin^2(3\Pi x_i + 1)\right] \\ + (x_n - 1)^2\left[1 + \sin^2(2\Pi x_n)\right] \end{matrix}\right\} + \sum_{i=1}^{n} u(x_i, 5, 100, 4)$	30, [–50, 50]

Table 4: Fixed-dimensional multimodal benchmark functions

Function	Formulation	Dim, limits
Foxholes	$f_{14} = \left(\frac{1}{500} + \sum_{j=1}^{25} \frac{1}{j + \sum_{i=1}^{2} \left(x_i - a_{ij} \right)^6} \right)^{-1}$	2, [–65.536, 65.536]
Kowalik	$f_{15} = \sum_{i=1}^{11} \left[a_i - \frac{x_1 \left(b_i^2 + b_i x_2 \right)}{b_i^2 + b_i x_3 + x_4} \right]^2$	4, [–5, 5]
Six-hump Camel-Back	$f_{16}(x) = 4x_1^2 - 2.1x_1^4 + \frac{1}{3}x_1^6 + x_1 x_2 + 4x_2^4$	2, [–5, 5]
Branin	$f_{17}(x) = \left(x_2 - \frac{5.1}{4\pi^2} x_1^2 + \frac{5}{\pi} x_1 - 6 \right)^2 + 10 \left(1 - \frac{1}{8\pi} \right) \cos x_1 + 10$	2, [–5, 5]
Goldstein-Price	$f_{18}(x) = \left[1 + (x_1 + x_2 + 1)^2 \left(19 - 14x_1 + 3x_1^2 - 14x_2 + 6x_1 x_2 + 3x_2^2 \right) \right] \times \left[30 + (2x_1 - 3x_2)^2 \left(18 - 32x_1 + 12x_1^2 + 48x_2 - 36x_1 x_2 + 27x_2^2 \right) \right]$	2, [–5, 5]
Hartman 3	$f_{19}(x) = -\sum_{i=1}^{4} c_i \exp \left(-\sum_{j=1}^{3} a_{ij} \left(x_j - p_{ij} \right)^2 \right)$	3, [–5, 5]
Hartman 6	$f_{20}(x) = -\sum_{i=1}^{4} c_i \exp \left(-\sum_{j=1}^{6} a_{ij} \left(x_j - p_{ij} \right)^2 \right)$	6, [–5, 5]
Shekel5	$f_{21}(x) = -\sum_{i=1}^{5} \left[(X - a_i)(X - a_i)^T + c_i \right]^{-1}$	3, [–5, 5]
Shekel7	$f_{22}(x) = -\sum_{i=1}^{7} \left[(X - a_i)(X - a_i)^T + c_i \right]^{-1}$	3, [–5, 5]
Shekel10	$f_{23}(x) = -\sum_{i=1}^{10} \left[(X - a_i)(X - a_i)^T + c_i \right]^{-1}$	3, [–5, 5]

For the analysis, 500 iterations have been considered. All the commonly used parametric values such as dimensions and limits are specified in Tables 2– 4. 30 individuals have evaluated each benchmark function runs for all the algorithms which are used for the comparison purpose. The best, worst, average and standard deviation values are obtained and recorded in Table 5. For the Unimodal test functions, the obtained values suggest that the proposed IHHO-PSO is com-

Table 5: Statistical results obtained by the proposed algorithm on the benchmark functions

		GWO	HHO	BMO	GWOPSO	HHOPSO
F1	Avg	9.38E–28	9.27E–96	0	2175.333885	1.71E–08
	SD	1.36E–27	4.31E–95	0	7820.382047	9.23E–08
	Best	5.52E–30	7.52E–117	0	2.55E–17	1.45E–115
	Worst	6.68E–27	2.36E–94	0	34228.90122	5.06E–07
F2	Avg	9.30E–17	4.79E–52	5.29E–284	60815.92213	6.57E–05
	SD	6.67E–17	1.34E–51	0	333085.8782	0.000341101
	Best	9.18E–18	1.49E–58	8.88577637208627E–310	2.58E–09	6.53E–59
	Worst	3.45E–16	6.10E–51	1.23E–282	1824389.529	0.00186946
F3	Avg	9.73E–06	1.06E–74	0	7416.94505	1.25E–08
	SD	2.00E–05	5.77E–74	0	17450.61714	6.84E–08
	Best	8.50E–09	1.48E–104	0	7.91E–05	1.87E–96
	Worst	9.32E–05	3.16E–73	0	69639.88128	3.74E–07
F4	Avg	6.82E–07	2.59E–49	2.30E–289	16.75227517	2.30E–06
	SD	7.21E–07	9.62E–49	0	24.1735725	1.25E–05
	Best	4.92E–08	1.12E–54	9.63E–307	0.000116378	2.19E–54
	Worst	2.98E–06	5.07E–48	5.21E–288	73.82112816	6.87E–05
F5	Avg	27.27335576	0.02023205	27.69896842	343944.1047	0.469940134
	SD	0.832761929	0.03078866	0.305122303	1560701.985	1.734166842
	Best	25.8456032	0.000143426	27.07196761	25.84274208	0.000341258
	Worst	28.77927397	0.122537827	28.50526373	8545455.147	7.133649141
F6	Avg	0.71632315	0.000144625	0.528164743	1026.450969	0.01146362
	SD	0.45463702	0.000163886	0.400459422	3706.041672	0.057157555
	Best	5.50E–05	1.21E–06	0.06195173	2.45E–05	2.01E–06
	Worst	2.262682171	0.00051295	1.512015995	17549.82006	0.313061157
F7	Avg	0.002388392	8.14E–05	3.79E–05	0.397959654	0.000651567
	SD	0.001209963	8.50E–05	3.62E–05	1.289519237	0.002859843
	Best	0.000813406	8.04E–06	7.19E–07	0.003197709	3.82E–06
	Worst	0.006020867	0.000437832	0.000190649	6.88743368	0.01578097
F8	Avg	–5905.414991	–12561.90943	–1636.212471	–6905.629111	–12528.95676
	SD	627.8338251	39.70150355	90.61695289	1490.791933	216.2809718
	Best	–7436.358621	–12569.48662	–1761.298102	–8932.098162	–12569.48639
	Worst	–4790.938625	–12351.72276	–1415.605532	–2315.740777	–11383.84671
F9	Avg	3.814339421	0	0	88.72394821	7.03E–08
	SD	3.812314812	0	0	99.16770416	3.85E–07
	Best	5.68E–14	0	0	10.22186414	0
	Worst	13.77399361	0	0	339.4267782	2.11E–06

Table 5 [cont.]

		GWO	HHO	BMO	GWOPSO	HHOPSO
F10	Avg	1.08E–13	8.88E–16	8.88E–16	5.759560777	1.24E–07
	SD	2.28E–14	0	0	6.045699968	6.80E–07
	Best	7.55E–14	8.88E–16	8.88E–16	7.23E–10	8.88E–16
	Worst	1.86E–13	8.88E–16	8.88E–16	18.6449237	3.72E–06
F11	Avg	0.004164123	0	0	26.54555287	2.89E–16
	SD	0.008941517	0	0	80.71234706	1.12E–15
	Best	0	0	0	2.55E–15	0
	Worst	0.033709471	0	0	308.4160995	5.88E–15
F12	Avg	0.040450313	9.31E–06	0.015325987	8011457.955	1.03E–05
	SD	0.018456931	1.22E–05	0.009018127	26100498.22	1.17E–05
	Best	0.012018569	2.36E–07	0.002192957	2.00E–05	1.58E–09
	Worst	0.092796986	4.81E–05	0.035769846	122729835.9	4.73E–05
F13	Avg	0.616770541	0.000113679	2.96858158	17554896.53	0.000377471
	SD	0.251937258	0.00017407	0.001868752	46410306.43	0.000895519
	Best	0.121838406	1.92E–06	2.966454983	0.000271301	1.58E–08
	Worst	1.138333421	0.000825297	2.974023571	191807228.4	0.004536553
F14	Avg	4.339078011	1.19680925	8.277217133	3.920017549	1.558402718
	SD	4.037241048	0.404408084	4.507573558	4.934721128	1.313623181
	Best	0.998003838	0.998003838	0.998003838	0.998003838	0.998003838
	Worst	12.67050581	1.9920309	12.67050581	17.3744065	5.928845125
F15	Avg	0.005149142	0.000377167	0.00046399	0.003256876	0.00038934
	SD	0.008543428	0.000206434	0.000176996	0.006840029	0.00020549
	Best	0.000308071	0.00030774	0.000307515	0.000307494	0.000311235
	Worst	0.020363344	0.00145345	0.000830685	0.020363407	0.001447517
F16	Avg	–1.031628434	–1.031628453	–1.03162747	–1.031208345	–1.031628034
	SD	1.51E–08	9.90E–10	5.39E–06	0.001108392	2.07E–06
	Best	–1.031628453	–1.031628453	–1.031628453	–1.031628453	–1.031628453
	Worst	–1.031628387	–1.03162845	–1.031598955	–1.027214797	–1.031617124
F17	Avg	0.397893203	0.397899742	0.397887358	0.397983122	0.397891509
	SD	1.72E–05	4.75E–05	0	0.000364677	1.15E–05
	Best	0.397887487	0.397887358	0.397887358	0.397887358	0.397887358
	Worst	0.397982038	0.398141499	0.397887358	0.399848783	0.397943231

Table 5 [cont.]

		GWO	HHO	BMO	GWOPSO	HHOPSO
F18	Avg	3.00003988	3.000000289	3	3.000265303	3.000000108
	SD	4.64E–05	9.87E–07	6.56E–15	0.00130654	2.24E–07
	Best	3.000000001	3	3	3.000000039	3
	Worst	3.000205112	3.00000529	3	3.007180979	3.00000093
F19	Avg	–3.861321243	–3.859660551	–0.300478907	–3.86041374	–3.859904889
	SD	2.46E–03	3.00E–03	2.26E–16	0.003290596	3.89E–03
	Best	–3.862781778	–3.862762447	–0.300478907	–3.862782145	–3.862782137
	Worst	–3.854983481	–3.853187491	–0.300478907	–3.854213761	–3.849749026
F20	Avg	–3.261080971	–3.057717761	–3.268148994	–3.154517011	–3.197437677
	SD	0.073570956	0.116002113	0.1136698	0.155549674	0.107045792
	Best	–3.321992413	–3.196957383	–3.321995172	–3.321995162	–3.321995165
	Worst	–3.135607765	–2.75707919	–2.840421628	–2.634700692	–2.932046217
F21	Avg	–9.644646076	–5.541379996	–5.055197729	–7.677879724	–5.370760891
	SD	1.546066435	1.498314393	9.03E–16	3.343400911	1.211725964
	Best	–10.15292324	–10.11786015	–5.055197729	–10.15319948	–10.00244381
	Worst	–5.055154258	–5.03553484	–5.055197729	–0.881395173	–5.036496344
F22	Avg	–9.970860477	–5.210087436	–5.26484745	–7.597252372	–5.388475643
	SD	1.666883601	0.985343965	0.970430863	3.268174922	1.377470348
	Best	–10.40244611	–10.25384795	–10.40294057	–10.40293646	–10.40294057
	Worst	–2.765712451	–3.703687412	–5.087671825	–2.751599985	–3.670041769
F23	Avg	–10.53443098	–5.462781772	–5.128480787	–9.047832458	–5.984680012
	SD	0.001087681	1.285594938	4.12E–15	3.035439212	1.959464983
	Best	–10.53588389	–10.32344028	–5.128480787	–10.53640962	–10.53640064
	Worst	–10.53159227	–5.116340478	–5.128480787	–1.664350542	–5.114448853

parable with the results obtained for the HHO, but the performance is superior as compared to other algorithms [61]. Similar is the case with the Multimodal test functions. However, for some functions with multiple global optima, the values obtained are less significant to that of HHO. The convergence characteristics in Fig. 1, as observed from the plot suggests a better convergence feature and also has small convergence time as compared with the other proposed algorithm. Hence IHHO-PSO offers a promising performance for both unimodal and multimodal function and thus can be positively implemented for the optimization problems.

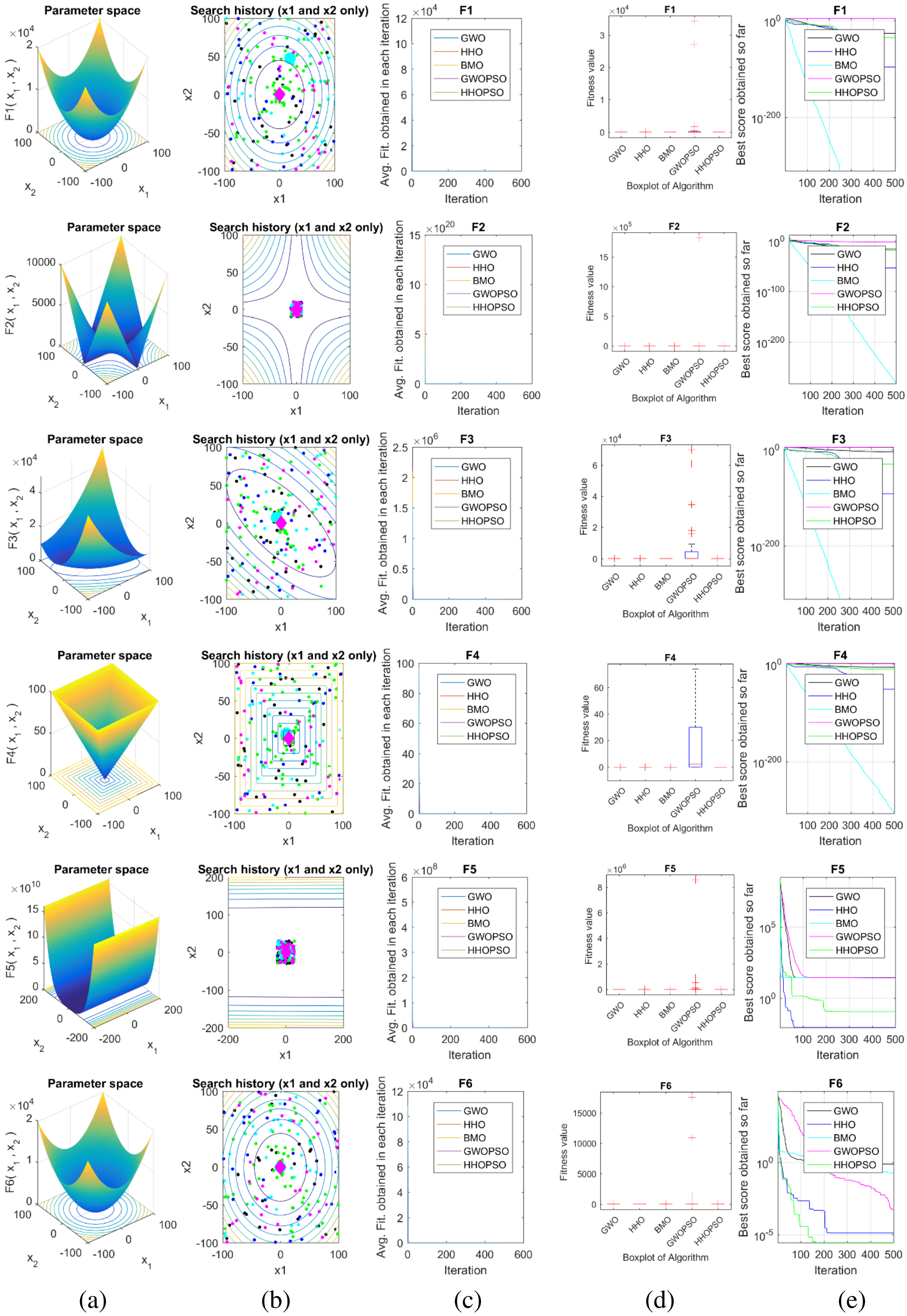

Parameter space
Search history (x1 and x2 only)
F1
F2
F3
F4
F5
F6
F1(x1 , x2)
F2(x1 , x2)
F3(x1 , x2)
F4(x1 , x2)
F5(x1 , x2)
F6(x1 , x2)
x1
x2
Avg. Fit. obtained in each iteration
Iteration
GWO
HHO
BMO
GWOPSO
HHOPSO
Fitness value
Boxplot of Algorithm
Best score obtained so far
(a)
(b)
(c)
(d)
(e)

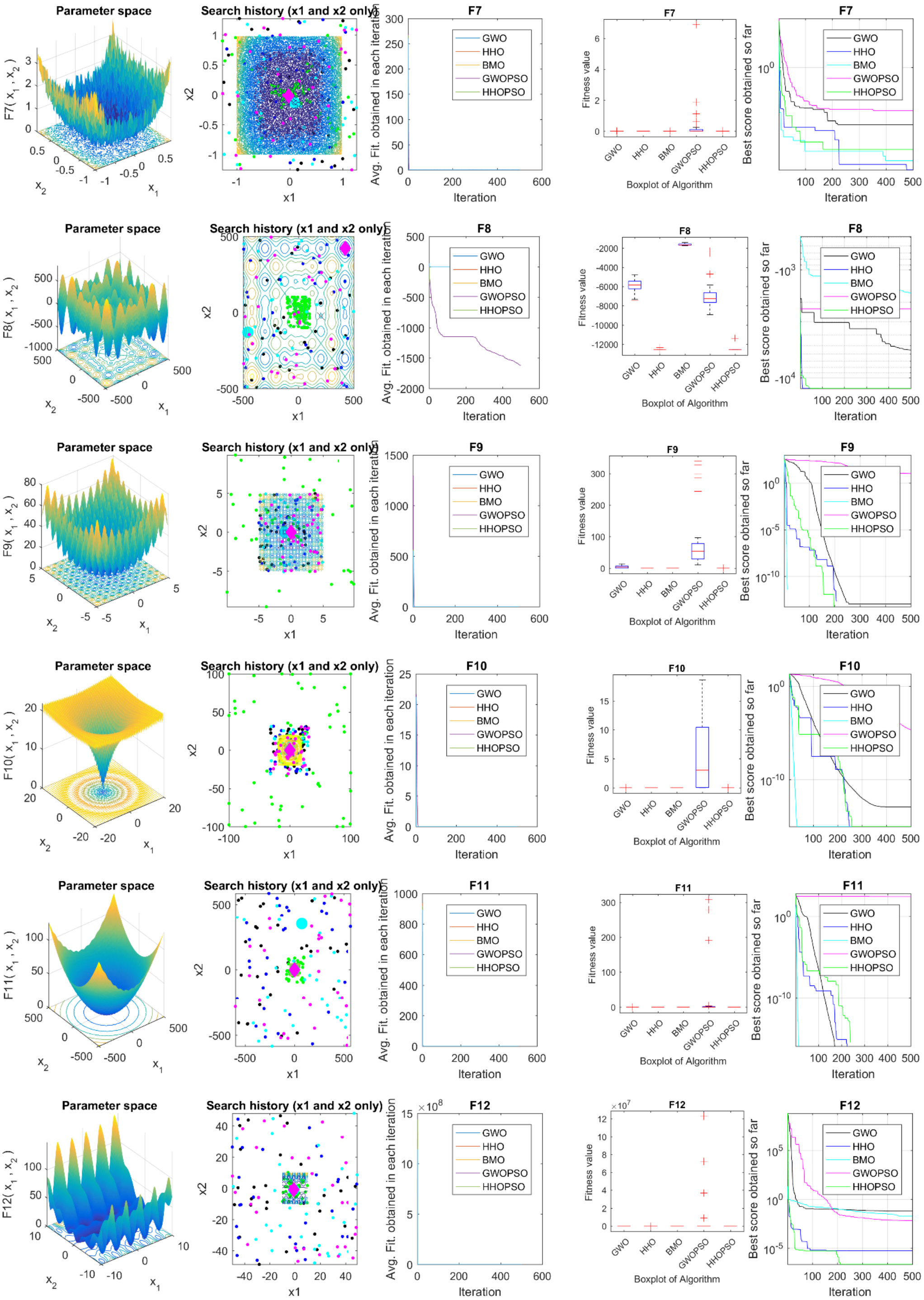
Parameter space
Search history (x1 and x2 only)
Avg. Fit. obtained in each iteration
Iteration
Boxplot of Algorithm
Fitness value
Best score obtained so far
F7
F8
F9
F10
F11
F12
GWO
HHO
BMO
GWOPSO
HHOPSO

(a) (b) (c) (d) (e)

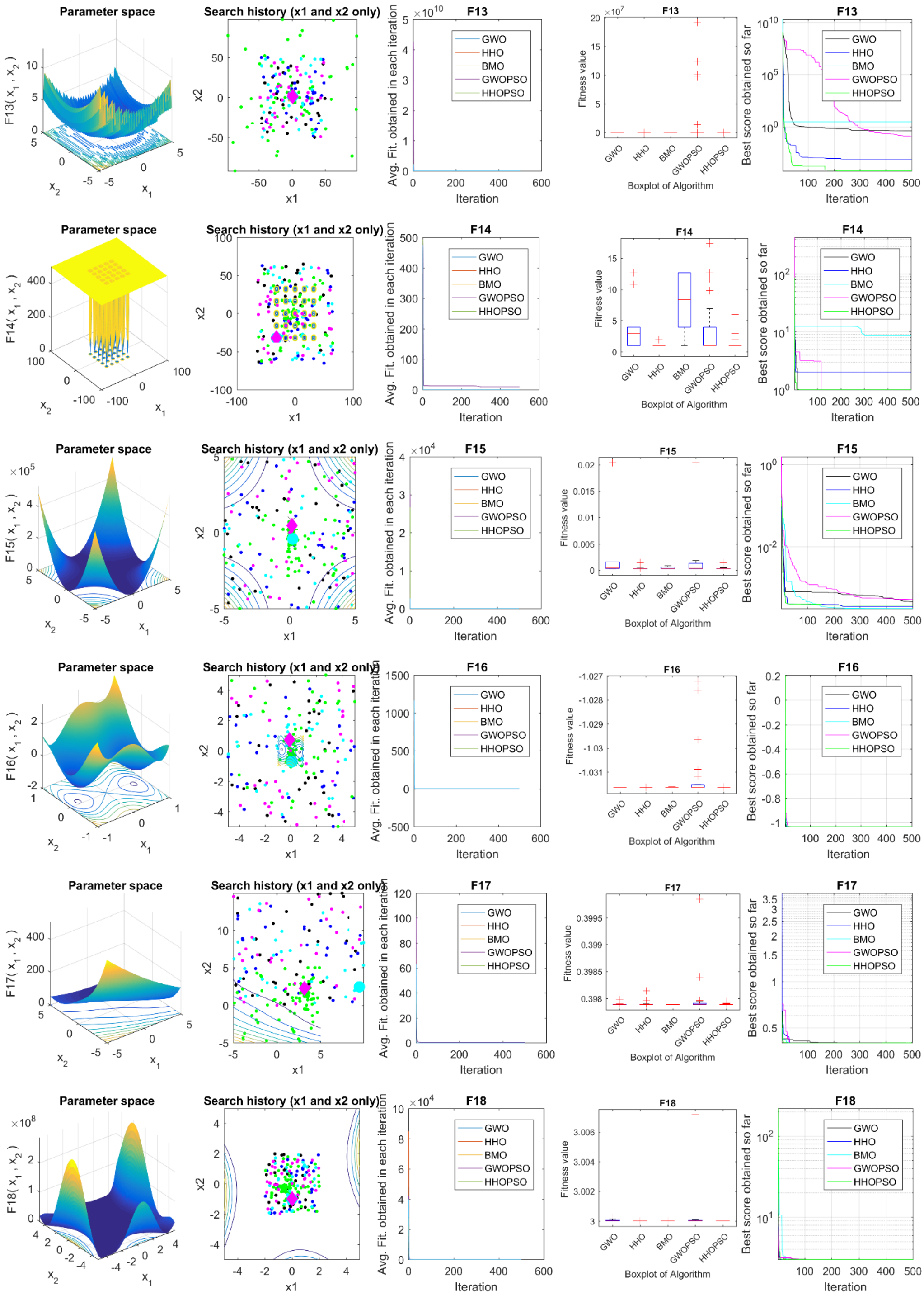
Parameter space
Search history (x1 and x2 only)
F13
F14
F15
F16
F17
F18
Avg. Fit. obtained in each iteration
Iteration
Fitness value
Boxplot of Algorithm
Best score obtained so far
GWO
HHO
BMO
GWOPSO
HHOPSO
x1
x2

(a) (b) (c) (d) (e)

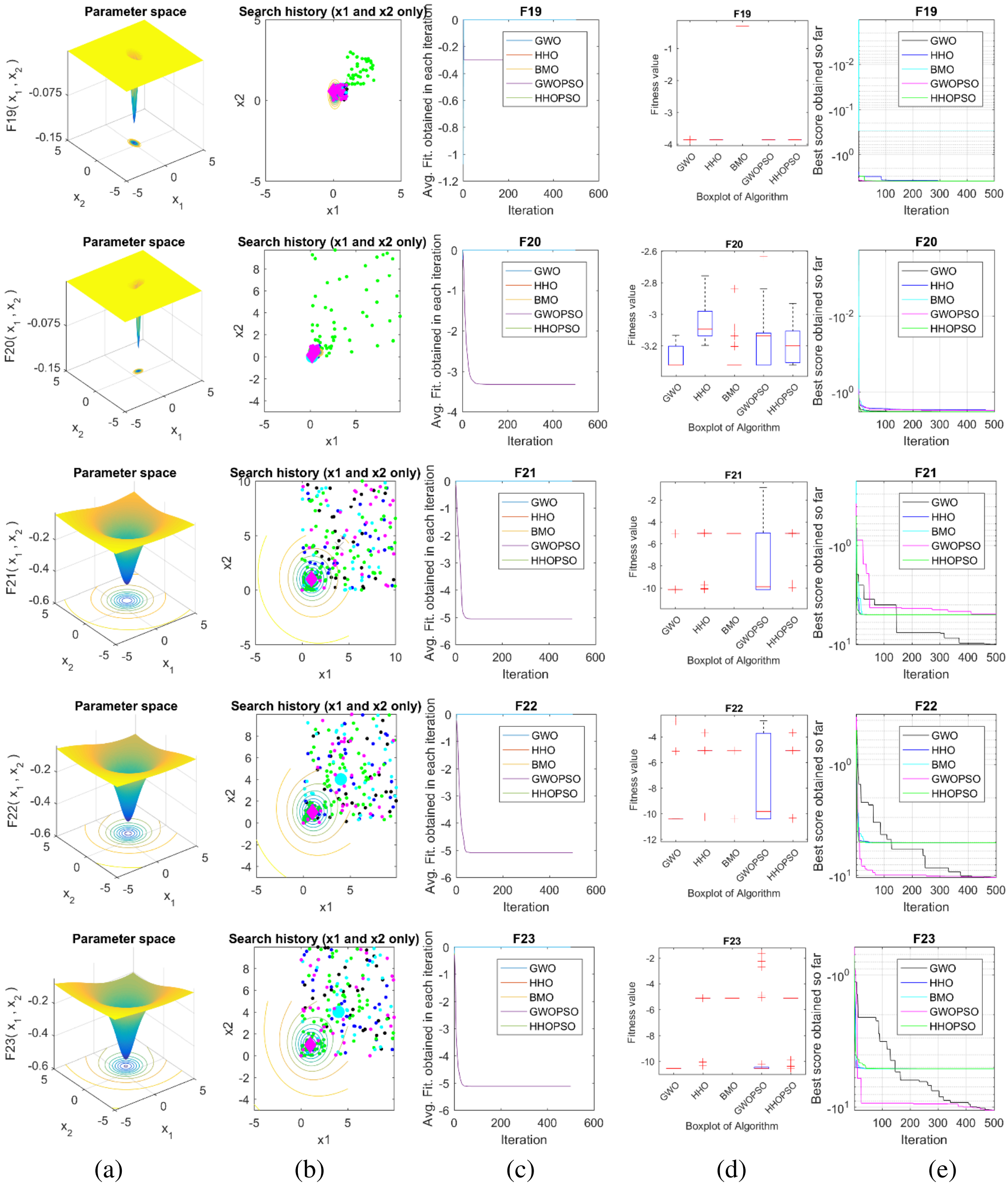

Figure 1: Benchmark functions from F1-F23 (a) 2D Function plot, (b) Search space with the proposed algorithms, (c) Average fitness value over the iterations, (d) Boxplot with the proposed algorithms, (e) Convergence characteristics with the proposed algorithms

In the next stage, we have used the IHHO-PSO for the optimization of controller time constants and gains for the FACTS based power system stabilizers. In recent years we have seen that the production and consumption of energy have exponentially increased. We always have a shortage of production as the demand increases with increase in population and industrialization. This shortage usually leads to load shedding, heavy loading of transmission lines, unbalance of active and reactive power. The cumulative effect leads to two significant problems in the power system, voltage instability and low-frequency oscillation [62] which is mainly due to unbalanced reactive supply. So, here we have used IHHO-PSO to study its effectiveness in optimizing the controller parameters for various loading conditions, i.e. light loading, nominal loading and heavy loading. Also, the eigenvalues, damping ratio and frequency of oscillation are obtained and compared with the existing algorithm to prove its superiority. However, the proposed approach adds the flexibility to the heuristic methods available in the literature [63].

4. Implementation of proposed algorithms for power system stability enhancement

The performance of the proposed algorithms has been applied to the most predominant engineering problem by considering a case study of a two area electric power system connected with a STATCOM in the middle of the transmission line as shown in Fig. 2 [64]. It consists of a two-machine system where two areas having its own local generation and load connected with an equivalent reactance value of the transmission lines where a STATCOM is connected in the middle of the transmission line. The complete system modelling is explained [65]. In the considered case study, PSS and STATCOM are employed to deal with the damping of undesirable system oscillations by controlling the excitation and providing adequate reactive power, respectively. PSS can be represented as a combination of

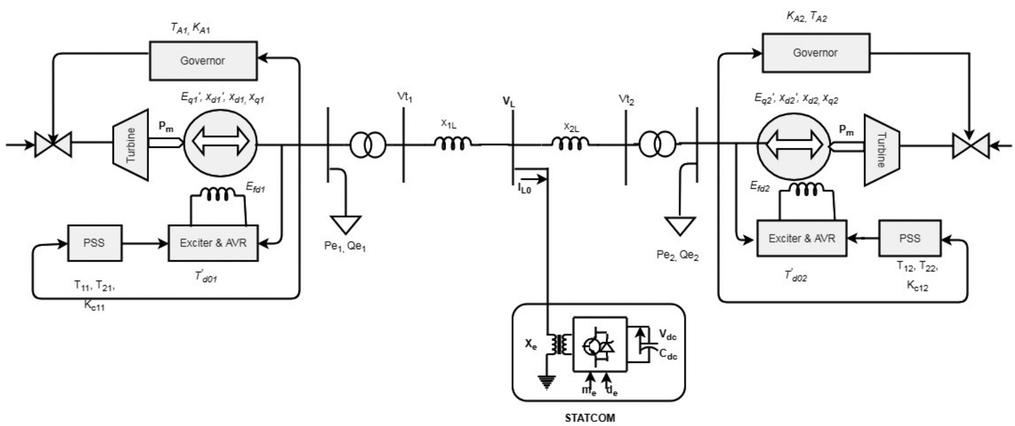

Figure 2: Schematic of the Mathematically modelled System to coordinate STATCOM and PSS controllers

two effects, namely, compensation and reset by which the field excitation can be controlled for the low-frequency oscillation. Figure 3 shows the block diagram of PSS, which consists of a compensation block and reset block. The control action for the field excitation by PSS depends on the speed variation in the synchronous machine due to the variation in the system operating conditions. PSS will provide u_{E1} and u_{E2} for the generator 1 and 2 respectively based on the parameters of compensation block of generator 1 and 2 (T_{11}, T_{21}, K_{c11} and T_{12}, T_{22}, K_{c12}).

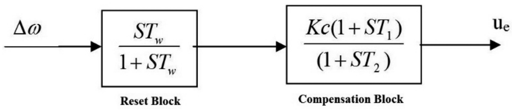

Figure 3: Block diagram of Power System Stabilizer

The function of the reset block is to terminate the compensation effect in steady-state and should not affect the compensation block, which can be achieved by choosing a large value of T_w. The STATCOM provides desired reactive power generation/absorption by means of Voltage Source Converter (VSC) which is supported by an energy storage device. The reactive power generation/absorption can be controlled by means of modulation ratio (m_e) of PWM and phase angle (d_e) of VSC. The direction of reactive power depends on the direction of STATCOM current between the utility bus and converter terminal bus, which further depends on the voltage difference between the converter terminal and utility bus. So it mainly used for dynamic compensation for providing voltage support, transient stability enhancement and to increase damping [66].

The state space representation of the considered system can be obtained from the dynamics of synchronous machine and exciter [67] given as (8)–(11).

$$\Delta\dot{\delta} = \omega_b \Delta\omega\,, \tag{8}$$

$$\Delta\dot{\omega} = \frac{(-\Delta P_e - D\Delta\omega)}{M}\,, \tag{9}$$

$$\Delta\dot{E}'_q = \frac{(-\Delta E_q + \Delta E_{fd})}{T'_{d0}}\,, \tag{10}$$

$$\Delta\dot{E}_{fd} = -\frac{1}{T_A}\Delta E_{fd} - \frac{K_A}{T_A}\Delta V_t\,, \tag{11}$$

where $\Delta\omega = (\omega - \omega_0)/\omega_0$.

For the STATCOM installed in two machine power network, without PSS as supplementary control, the state equations can be written as

$$\dot{X} = AX + BU\,, \tag{12}$$

where A is the state matrix, B is the STATCOM control input matrix. With the state variables $[\Delta\dot{\delta}_1\ \Delta\dot{\omega}_1\ \Delta\dot{E}'_{q1}\ \Delta\dot{E}_{fd1}\ \Delta\dot{V}_{dc}\ \Delta\dot{\delta}_2\ \Delta\dot{\omega}_2\ \Delta\dot{E}'_{q2}\ \Delta\dot{E}_{fd2}]^T$ and the control variables of $[\Delta m_e\ \Delta d_e]^T$.

For the system with supplementary control u_{E1} and u_{E2} the state space representation can be given as,

$$\dot{X} = AX + BU + B_E u_E = A_c X + B_c U\,, \tag{13}$$

where A is system state matrix, B is STATCOM control input matrix and B_E is supplementary control matrix. The consolidated system matrixes can be represented as,

$$A_c = \begin{bmatrix} A_{11} & \dots & A_{113} \\ \vdots & \ddots & \vdots \\ A_{131} & \dots & A_{1313} \end{bmatrix} \tag{14}$$

and

$$B_c = \Big[0\ 0;\ B_{21}\ B_{22};\ B_{31}\ B_{32};\ B_{41}\ B_{42};\ B_{51}\ B_{52};\ B_{61}\ B_{61};\ B_{71}\ B_{72};\ 0\ 0;\\ B_{91}\ B_{92};\ B_{101}\ B_{102};\ B_{111}\ B_{112};\ B_{121}\ B_{122};\ B_{131}\ B_{132}\Big]. \tag{15}$$

Form the linear system equations as given in [64], the system constants can be given as follows:
$A_{12} = w_0$; $A_{21} = -K_{11}/M_1$; $A_{22} = -D_1/M_1$; $A_{23} = -K_{21}/M_1$;
$A_{25} = -Kqe_1/M_1$; $A_{31} = -K_{41}/Td0_{11}$; $A_{33} = -K_{31}/Td0_{11}$;
$A_{34} = 1/Td0_{11}$; $A_{35} = -Kqd_1/Td0_{11}$; $A_{41} = -Ka_1 \cdot K_{51}/Ta_1$;
$A_{43} = -Ka_1 \cdot K_{61}/Ta_1$; $A_{44} = -1/Ta_1$; $A_{45} = -Ka_1 \cdot Kvd_1/Ta_1$;
$A_{47} = Ka_1/Ta_1$; $A_{51} = K_{71}$; $A_{53} = K_{81}$; $A_{55} = -K_9$; $A_{58} = K_{72}$; $A_{510} = K_{82}$;
$A_{61} = -K_{11}/M_1$; $A_{62} = -D_1/M_1$; $A_{63} = -K_{21}/M_1$; $A_{65} = -Kqe_1/M_1$;
$A_{66} = -1/T_w$; $A_{71} = -KA_{11}\cdot K_{11}\cdot T_{11}/(M_1\cdot T_{21})$; $A_{72} = -D_1\cdot KA_{11}\cdot T_{11}/(M_1\cdot T_{21})$;
$A_{73} = -KA_{11} \cdot T_{11} \cdot K_{21}/(M_1 \cdot T_{21})$; $A_{75} = -Kqe_1 \cdot KA_{11} \cdot T_{11}/(M_1 \cdot T_{21})$;
$A_{76} = (KA_{11}/T_{21}) \cdot (1 - (T_{11}/T_w))$; $A_{77} = -1/T_{21}$; $A_{89} = w_0$; $A_{95} = -Kqe_2/M_2$;
$A_{98} = -K_{12}/M_2$; $A_{99} = -D_2/M_2$; $A_{910} = -K_{22}/M_2$; $A_{105} = -Kqd_2/Td0_{12}$;
$A_{108} = -K_{42}/Td0_{12}$; $A_{1010} = -K_{32}/Td0_{12}$; $A_{1011} = 1/Td0_{12}$;
$A_{115} = -Ka_2 \cdot Kvd_2/Ta_2$; $A_{118} = -Ka_2 \cdot K_{52}/Ta_2$; $A_{1110} = -Ka_2 \cdot K_{62}/Ta_2$;
$A_{1111} = -1/Ta_2$; $A_{1113} = Ka_2/Ta_2$; $A_{125} = -Kqe_2/M_2$; $A_{128} = -K_{12}/M_2$;
$A_{129} = -D_2/M_2$; $A_{1210} = -K_{22}/M_2$; $A_{1212} = -1/T_w$;
$A_{135} = -Kqe_2 \cdot KA_{12} \cdot T_{12}/(M_2 \cdot T_{22})$; $A_{138} = -KA_{12} \cdot K_{12} \cdot T_{12}/(M_2 \cdot T_{22})$;
$A_{139} = -D_2 \cdot KA_{12} \cdot T_{12}/(M_2 \cdot T_{22})$; $A_{1310} = -KA_{12} \cdot T_{12} \cdot K_{22}/(M_2 \cdot T_{22})$;
$A_{1312} = (KA_{12}/T_{22}) \cdot (1 - (T_{12}/T_w))$; $A_{1313} = -1/T_{22}$;
and zero for the remaining elements.
$B_{21} = -Kpe_1/M_1$; $B_{22} = -Kpde_1/M_1$; $B_{31} = -Kqe_1/Td0_{11}$;
$B_{32} = -Kqde_1/Td0_{11}$; $B_{41} = -Ka_1 \cdot Kve_1/Ta_1$; $B_{42} = -Ka_1 \cdot Kvde_1/Ta_1$;

$B_{51} = K_{Ae}$; $B_{52} = K_{Ade}$; $B_{61} = -Kpe_1/M_1$; $B_{62} = -Kpde_1/M_1$;
$B_{71} = -KA_{11} \cdot T_{11} \cdot Kpe_1/(M_1 \cdot T_{21})$; $B_{72} = -KA_{11} \cdot T_{11} \cdot Kpde_1/(M_1 \cdot T_{21})$;
$B_{91} = -Kpe_2/M_2$; $B_{92} = -Kpde_2/M_2$; $B_{101} = -Kqe_2/Td0_{12}$;
$B_{102} = -Kqde_2/Td0_{12}$; $B_{111} = -Ka_2 \cdot Kve_2/Ta_2$; $B_{112} = -Ka_2 \cdot Kvde_2/Ta_2$;
$B_{121} = -Kpe_2/M_2$; $B_{122} = -Kpde_2/M_2$; $B_{131} = -KA_{12} \cdot T_{12} \cdot Kpe_2/(M_2 \cdot T_{22})$;
$B_{132} = -KA_{12} \cdot T_{12} \cdot Kpde_2/(M_2 \cdot T_{22})$;
where,

$$K_{11} = \frac{(V_{t1d} - x'_{d1} I_{1Lq})(x_{de1} - x_{dt1}) V_{t2} \sin(\delta_1 - \delta_2)}{x_{dee1}} + \frac{(V_{t1q} + x_{q1} I_{1Ld})(x_{qt1} - x_{qe1}) V_{t2} \cos(\delta_1 - \delta_2)}{x_{qee1}};$$

$$K_{21} = \left(I_{1Lq} + \frac{V_{t1d}(x_{2L} + x_e)}{x_{dee1}} \right);$$

$$K_{31} = 1 + \frac{(x'_{d1} - x_{d1})(x_{2L} + x_e)}{x_{dee1}};$$

$$K_{41} = \frac{-(x'_{d1} - x_{d1})(x_{de1} - x_{dt1}) V_{t2} \sin(\delta_1 - \delta_2)}{x_{dee1}};$$

$$K_{pe1} = \frac{(V_{t1d} - x'_{d1} I_{1Lq})(x_{bd1} - x_{de1}) V_{dc} \sin d_e}{2x_{dee1}} + \frac{(V_{t1q} + x_{q1} I_{1Ld})(x_{bq1} - x_{qe1}) V_{dc} \cos d_e}{2x_{qee1}};$$

$$K_{pde1} = \frac{(V_{t1d} - x'_{d1} I_{1Lq})(x_{bd1} - x_{de1}) m_e V_{dc} \cos d_e}{2x_{dee1}} + \frac{(V_{t1q} + x_{q1} I_{1Ld})(-x_{bq1} + x_{qe1}) m_e V_{dc} \sin d_e}{2x_{qee1}};$$

$$K_{pd1} = \frac{(V_{t1d} - x'_{d1} I_{1Lq})(x_{bd1} - x_{de1}) m_e \sin d_e}{2x_{dee1}} + \frac{(V_{t1q} + x_{q1} I_{1Ld})(x_{bq1} - x_{qe1}) m_e \cos d_e}{2x_{qee1}};$$

$$K_{51} = \frac{(V_{t1d}/V_{t1}) x_{q1} (x_{qt1} - x_{qe1}) V_{t2} \cos(\delta_1 - \delta_2)}{x_{qee1}} - \frac{(V_{t1q}/V_{t1}) x'_{d1} (x_{de1} - x_{dt1}) V_{t2} \cos(\delta_1 - \delta_2)}{x_{dee1}};$$

$$K_{61} = \frac{(V_{t1q}/V_{t1})(x_{dee1} + x'_{d1}(x_{2L} - x_e))}{x_{dee1}};$$

$$K_{71} = \left(\frac{3}{4C_{dc}}\right)\left\{\frac{m_e V_{t2}\sin(\delta_1-\delta_2)(\cos d_e)x_{de1}}{x_{dee1}} - \frac{m_e V_{t2}\cos(\delta_1-\delta_2)(\sin d_e)x_{qe1}}{x_{qee1}}\right\};$$

$$K_{81} = \left(-\frac{3}{4C_{dc}}\right)\frac{x_{2L}m_e\cos d_e}{x_{dee1}};$$

similarly, constants with respective to generator 2 can also be written as:

$$K_9 = \left(\frac{3}{4C_{dc}}\right)\left\{\begin{array}{l}\dfrac{m_e\sin d_e(m_e\cos d_e)x_{bd1}}{2x_{dee1}} + \dfrac{m_e\cos d_e(m_e\sin d_e)x_{bq1}}{2x_{qee1}}\\ +\dfrac{m_e\sin d_e(m_e\cos d_e)x_{bd2}}{2x_{dee2}} + \dfrac{m_e\cos d_e(m_e\sin d_e)x_{bq2}}{2x_{qee2}}\end{array}\right\};$$

$$K_{ce} = \left(\frac{3}{4C_{dc}}\right)\left\{\begin{array}{l}\dfrac{V_{dc}\sin d_e(m_e\cos d_e)x_{bd1}}{2x_{dee1}} + \dfrac{V_{dc}\cos d_e(m_e\sin d_e)x_{bq1}}{2x_{qee1}}\\ +\dfrac{V_{dc}\sin d_e(m_e\cos d_e)x_{bd2}}{2x_{dee2}} + \dfrac{V_{dc}\cos d_e(m_e\sin d_e)x_{bq2}}{2x_{qee2}}\end{array}\right\};$$

$$K_{cde} = \left(\frac{3m_e}{4C_{dc}}\right)\left(I_{L0q}\cos d_e - I_{L0d}\sin d_e\right) + \left(\frac{3}{4C_{dc}}\right)\left\{\begin{array}{l}\dfrac{m_eV_{dc}\cos d_e(m_e\cos d_e)x_{bd1}}{2x_{dee1}} - \dfrac{m_eV_{dc}\sin d_e(m_e\sin d_e)x_{bq1}}{2x_{qee1}}\\ +\dfrac{m_eV_{dc}\cos d_e(m_e\cos d_e)x_{bd2}}{2x_{dee2}} - \dfrac{m_eV_{dc}\sin d_e(m_e\sin d_e)x_{bq2}}{2x_{qee2}}\end{array}\right\}.$$

From Fig. 3, it has been observed that the controlling action by PSS is produced through a compensation block, based on the generator speed variation. The magnitude of the control signal is based on the tuning of gain and time constants in the compensation transfer function. Whereas, STATCOM will offer damping nature to the system oscillations by providing adequate reactive power at the utility bus [68] based on the magnitude of STATCOM current. Where the reactive power is controlled by the tuning modulation index and phase angle of voltage source converter [64]. For the designed power system, the coordination among the PSSs and STATCOM can be achieved by simultaneous tuning of the controller parameters subjected to the boundary limits as in (16).

$$\left.\begin{array}{r} T_{1i,\min} \leqslant T_{1i} \leqslant T_{1i,\max} \\ T_{2i,\min} \leqslant T_{2i} \leqslant T_{2i,\max} \\ d_{e,\min} \leqslant d_e \leqslant d_{e,\max} \\ m_{e,\min} \leqslant m_e \leqslant m_{e,\max} \\ Kc_{1i,\min} \leqslant Kc_{1i} \leqslant Kc_{1i,\max} \end{array}\right\}, \tag{16}$$

where T_{1i}, T_{2i}, K_{c1i} are the time constants and gain of PSS respectively of i^{th} generator and m_e and d_e are the PWM modulation index and phase angle of VSC based STATCOM. The control parameter limits have been given as follows,

Table 6: Limits of control parameters

	PSS 1			PSS 2			STATCOM	
	T_{11}	T_{21}	Kc_{11}	T_{12}	T_{22}	Kc_{12}	m_e	d_e
Min. limit	0.01	0.01	0.1	0.01	0.01	0.1	0	0
Max. limit	2	2	50	2	2	50	1	1

The desirable feature of the system for the stable mode of operation is, it should have better damping nature by bearing higher damping ratio for the system poles and faster decay to its nominal value from its fluctuating state. To achieve the system characteristics, the system poles desirably in the location as shown in Fig. 4. For the considered system, the system poles can be obtained by its eigenvalues as given as, $\lambda_i = \mathrm{Re}\,[\lambda_i] + j\mathrm{Im}\,[\lambda_i]$, $i = 1, 2, 3, \ldots, s$ where s is the number of system states. And the corresponding damping ratio and natural frequency of oscillation is given as in (17), (18).

Damping ratio

$$(\xi_i) = \frac{-\mathrm{Re}\,[\lambda_i]}{\sqrt{(\mathrm{Re}\,[\lambda_i])^2 + (\mathrm{Im}\,[\lambda_i])^2}}\,. \tag{17}$$

Frequency of oscillation

$$f_{\mathrm{osc}} = \frac{|\mathrm{Im}\,[\lambda_i]\,|}{2\Pi}\,. \tag{18}$$

The objective can be mathematically expressed in (19).

$$J = J_1 + \alpha J_2 = \left\{\sum_{i=1}^{s} (\sigma_0 - \mathrm{Re}\,[\lambda_i])^2 + \alpha \sum_{i=1}^{s} (\xi_0 - \xi_i)^2\right\} \tag{19}$$

where s = no. of system state variables, decrement ratio (σ_0) and damping factor (ξ_0). The factors for the considered test system have been considered from [3].

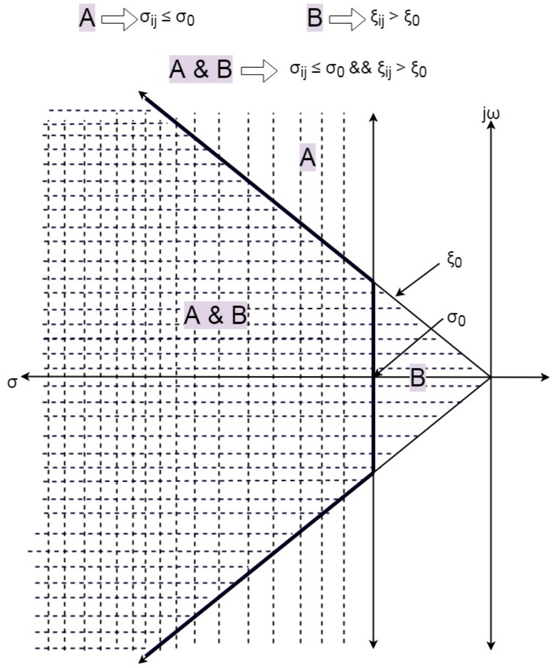

Figure 4: Operating region for the corresponding objective function

In (19), the function J_1 corresponds to the shifting the poles towards the left-hand side of s-plane based on the selection of σ_0 and J_2 corresponds to the improvement in the damping ratio of the low-frequency oscillations depending on the preference of ξ_0 which are represented as portion A and B respectively in Fig. 3. Where α value serves as the weightage for the individual objective to balance between J_1 and J_2. Here, as the J_2 function deals with the lower damping ratios, its magnitude is relatively low compared to J_1.

5. Results and analysis

For the considered case study, the coordination among the controllers has been achieved by tuning the controller parameters within the inequality constraints and listed in Table 7 by using the proposed metaheuristic algorithms. The tuned parameters and the statistical analysis have been presented under different loading conditions. The statistical analysis consists of the convergence characteristics of the considered algorithms w.r.t. the iterations and the execution time of the algorithms under different loading conditions, where, ‘TOE’ represents the time of execution of the respective algorithm in seconds for the given loading condition and ‘ObjFun’ represents the minimized value of the objective function.

Table 7: Tuned parameters of controller parameters with the proposed metaheuristic optimization algorithms

Nominal Load Condition						
	GWO	HHO	BMO	GWO-PSO	HHO-PSO	Convergence characteristics of the proposed optimization algorithms
T_{11}	2.0000	1.8683	2.0000	1.9945	1.2437	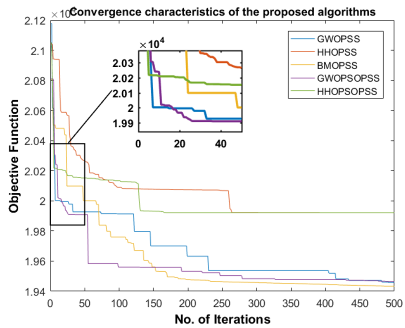
T_{21}	0.2853	0.3374	0.3316	0.3634	0.3026	
K_1	6.46	5.09	6.41	8.53	9.43	
T_{12}	1.9488	2.0000	2.0000	1.6592	1.9998	
T_{22}	0.2055	0.1905	0.2279	0.2507	0.2124	
K_2	4.25	4.13	3.96	5.03	4.99	
m_e	0.5859	0.7200	0.5925	0.5881	0.7163	
d_e	0.8633	1.0000	0.8633	0.8633	0.9999	
TOE (Sec)	21.96	51.89	44.25	21.59	49.48	
Obj Fun	19457.36	19922.25	19432.89	19464.85	19922.06	

Light Load Condition						
	GWO	HHO	BMO	GWO-PSO	HHO-PSO	Convergence characteristics of the proposed optimization algorithms
T_{11}	2.0000	1.8526	2.0000	1.9773	1.9945	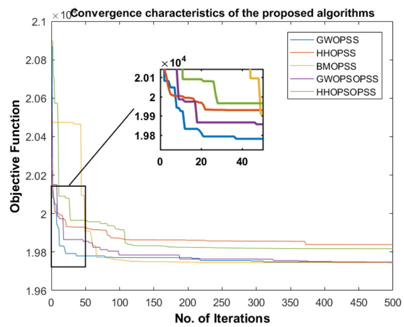
T_{21}	0.6417	0.5741	0.6042	0.6422	0.3784	
K_1	20.68	32.19	19.31	21.54	17.88	
T_{12}	2.0000	1.3458	2.0000	2.0000	0.8700	
T_{22}	0.3881	0.3179	0.3938	0.3817	0.2798	
K_2	8.21	8.11	7.81	7.92	15.51	
m_e	1.0000	0.8360	0.9868	0.9932	0.7868	
d_e	0.5553	0.2251	0.5378	0.5455	0.0735	
TOE (Sec)	19.86	50.01	40.82	20.17	46.84	
Obj Fun	19744.43	19838.75	19745.12	19747.44	19817.26	

Heavy Load Condition						
	GWO	HHO	BMO	GWO-PSO	HHO-PSO	Convergence characteristics of the proposed optimization algorithms
T_{11}	2.0000	0.7029	1.9999	2.0000	1.5917	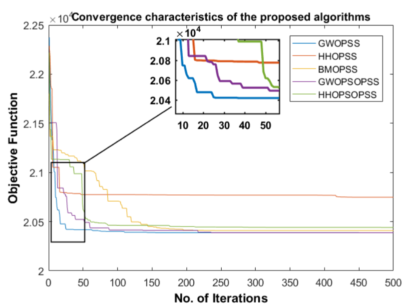
T_{21}	0.1289	0.2613	0.1265	0.1271	0.1394	
K_1	3.67	48.81	3.82	3.75	5.37	
T_{12}	2.0000	1.9536	2.0000	2.0000	1.3909	
T_{22}	0.1428	0.2267	0.1533	0.1471	0.1461	
K_2	5.00	10.27	5.81	5.10	8.57	
m_e	1.0000	0.9828	0.9364	1.0000	0.9156	
d_e	0.0003	0.1384	0.0540	0.0000	0.0116	
TOE (Sec)	20.49	48.15	42.08	19.49	46.07	
Obj Fun	20387.33	20748.76	20408.97	20387.61	20440.73	

Table 7 [cont.]

TOE	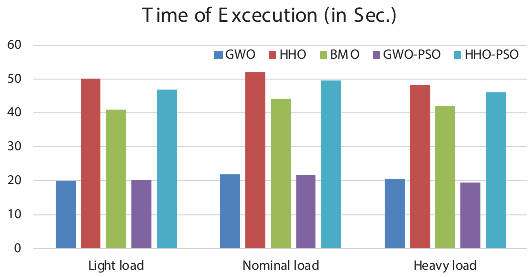

The performance of various optimization methods varies from case to case and in such a scenario different analysis has to be performed for the proposed algorithms on the modelled system under different operating conditions to comment on the suitability of the optimization algorithm. In this section, an eigenvalue analysis and damping nature of the system states under perturbation has been presented for the considered system under different loading conditions. Table 8 represents the system oscillating mode eigenvalues and their corresponding damping ratios with the proposed techniques under different loading conditions. Corresponding to the considered objective function, the system eigenvalues had higher negative real parts and positive damping ratios. The system is in a stable mode of operation for the various system operating conditions. From the magnitudes presented, it has been observed that IHHO-PSO has shown better magnitudes in respect of damping ratios and is expected to be more stable under the different operating environment in comparison with the other proposed optimization techniques. The total number of oscillating modes also been reduced with the proposed algorithm.

The system performance is further analyzed by considering the damping characteristics for the disturbance occurred during the operating condition. For the purpose of the study, we have assumed 10% perturbation to simulate the natural oscillating behaviour of the system at $t = 0$ sec. The damping nature obtained for the parameters of the two machines with the tuned parameters of the controller are shown in Figs. 5 to 7. Also, for the purpose of evaluation and analysis, we have considered torque angle, angular speed, generator internal voltage and generator field excitation as the system states which are studied. The variation in the states of these parameters is plotted w.r.t time for both the machines in the two – area system. The analysis has further been made more specific by considering all these system states for three different loading condition i.e. light loading, moderate loading and heavy loading. Figure 5 shows the variation of system states w.r.t time in the lightly loaded condition. The proposed metaheuristic IHHO-PSO gives a very satisfactory result for the torque angle deviation. The oscillations are minimum, and the time required for zero deviation is also less. However, for

Table 8: System eigen values with and corresponding damping ratios

	Light Load			Nominal load			Heavy load		
	Eigen Values	Freq	Damp	Eigen Values	Freq	Damp	Eigen Values	Freq	Damp
GWO	–0.4134 ±1.0497i	0.1670	0.3665	–0.0004 – 0.0010i	0.0002	0.3435	–1.9160 ±2.4776i	0.3942	0.6117
	–0.4249 ±1.1028i	0.1754	0.3595	–0.8650 + 1.6476i	0.2621	0.4649	–2.0844 ±2.5021i	0.3981	0.6401
	–2.6778 ±5.8845i	0.9362	0.4142	–0.5537 – 2.1144i	0.3364	0.2533	–3.6409 ±9.2747i	1.4755	0.3654
	–2.6291 ±5.9466i	0.9461	0.4044	–1.1344 – 2.6664i	0.4242	0.3915	–3.2880 ±10.3224i	1.6422	0.3035
				–1.1452 + 2.6655i	0.4241	0.3948			
				–2.9968 – 6.6161i	1.0526	0.4126			
				–3.3797 + 6.7827i	1.0791	0.446			
				–3.3753 – 6.7912i	1.0804	0.4451			
				–3.3960 + 7.0935i	1.1285	0.4318			
				–96.0620 – 0.0002i	3.2E–05	1			
HHO	–0.4676 ±0.9109i	0.1449	0.4567	–1.0286 ±2.2477i	0.3576	0.4161	–0.0398 ±0.0203i	0.0032	0.8908
	–0.7544 ±1.7496i	0.2783	0.3959	–1.1267 ±2.7008i	0.4297	0.385	–1.6036 ±1.1518i	0.1832	0.8122
	–2.7123 ±5.0629i	0.8055	0.4722	–2.5994 ±5.1619i	0.8212	0.4498	–1.3967 ±1.5778i	0.2510	0.6628
	–2.4228 ±7.9459i	1.2641	0.2917	–3.5703 ±7.1139i	1.1318	0.4486	–2.4613 ±11.8856i	1.8909	0.2028
							–1.9370 ±13.7476i	2.1871	0.1395
BMO	–0.4283 ±1.0974i	0.1746	0.3636	–0.0002 – 0.0006i	9.5E–05	0.2584	–0.0487 ±0.0087i	0.0014	0.9844
	–0.4375 ±1.1233i	0.1787	0.363	–0.8766 + 1.7049i	0.2712	0.4573	–1.9748 ±2.4463i	0.3892	0.6281
	–2.6364 ±5.6049i	0.8917	0.4256	–0.7241 – 1.9969i	0.3177	0.3409	–2.1128 ±2.4498i	0.3897	0.6531
	–2.6687 ±6.0508i	0.9626	0.4035	–1.3170 + 2.7135i	0.4317	0.4366	–3.7438 ±9.5286i	1.5159	0.3657
				–1.3105 – 2.7168i	0.4322	0.4345	–3.1470 ±10.9005i	1.7342	0.2774
				–2.7700 – 6.0887i	0.9687	0.4141			
				–2.9962 + 6.2857i	1.0000	0.4303			
				–3.0023 – 6.3257i	1.0064	0.4288			
				–3.0386 + 6.4247i	1.0221	0.4275			
				–95.9795 – 0.0001i	1.6E–05	1			
GWO-PSO	–0.3883 ±0.9926i	0.1579	0.3643	–0.0003 – 0.0009i	0.0001	0.318	–1.9314 ±2.4428i	0.3886	0.6202
	–0.4659 ±1.1795i	0.1876	0.3674	–0.0496 – 0.0001i	1.6E–05	1	–2.0189 ±2.4961i	0.3971	0.6289
	–2.7108 ±5.7405i	0.9133	0.427	–0.8633 + 1.4292i	0.2274	0.517	–3.7262 ±9.3983i	1.4952	0.3686
	–2.5969 ±6.1304i	0.9753	0.3901	–0.6642 – 1.7880i	0.2845	0.3482	–3.1958 ±10.3228i	1.6423	0.2957
				–1.4307 + 2.5895i	0.4120	0.4836			
				–1.4262 – 2.5925i	0.4124	0.482			
				–2.7013 – 6.1826i	0.9836	0.4004			
				–2.7040 + 6.1851i	0.9840	0.4006			
				–2.5443 – 6.8333i	1.0871	0.3489			
				–2.9610 + 7.1937i	1.1445	0.3806			
				–96.0766 – 0.0002i	3.2E–05	1			
IHHO-PSO	–0.6931 ±1.4456i	0.2300	0.4323	–0.8485 ±1.8968i	0.3018	0.4083	–0.0481 ±0.0101i	0.0016	0.9784
	–0.6935 ±1.4513i	0.2309	0.4311	–1.0663 ±2.4313i	0.3868	0.4017	–1.8893 ±2.4503i	0.3898	0.6106
	–2.7201 ±5.9494i	0.9465	0.4158	–2.9179 ±6.1888i	0.9846	0.4265	–2.2097 ±2.2862i	0.3637	0.695
	–2.8282 ±7.7012i	1.2252	0.3447	–3.3076 ±7.5223i	1.1967	0.4025	–3.4159 ±9.7660i	1.5537	0.3302
							–3.2163 ±11.1780i	1.7783	0.2765

angular speed deviation HHO shows smaller deviation, still the time required for zero deviation is almost comparable with that of IHHO-PSO. For the deviation in the generator internal voltage and field excitation IHHO-PSO outperforms other algorithms. The system states with nominal loadings are plotted in Fig. 6. For the torque angle deviation GWO-PSO shows minimum oscillation but it fails to reach zero deviation. However, IHHO-PSO gives more satisfactory results with zero deviation and a small oscillating time. Results for angular speed deviation is almost similar for all the algorithms. In the case of generator internal voltage and field excitation, the superiority of IHHO-PSO is distinctly visible. It gives minimum fluctuations and produces almost zero deviation. The system states

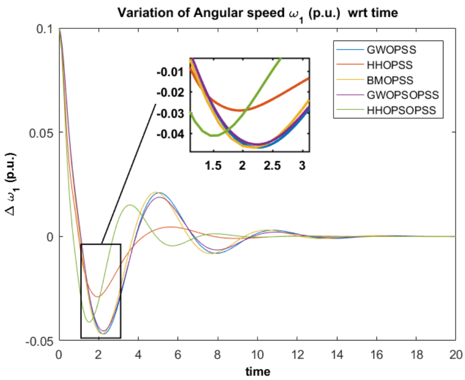

(a)

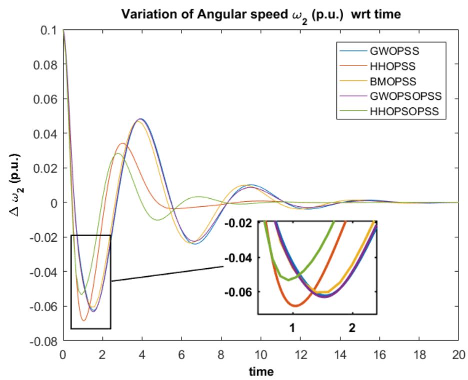

(b)

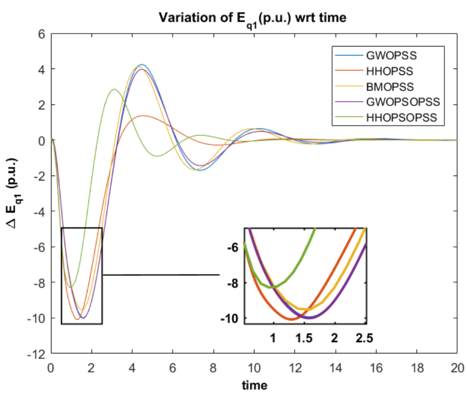

(c)

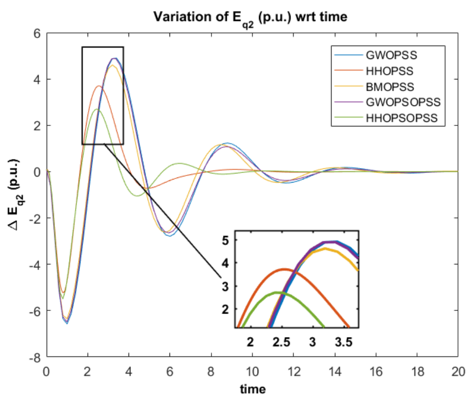

(d)

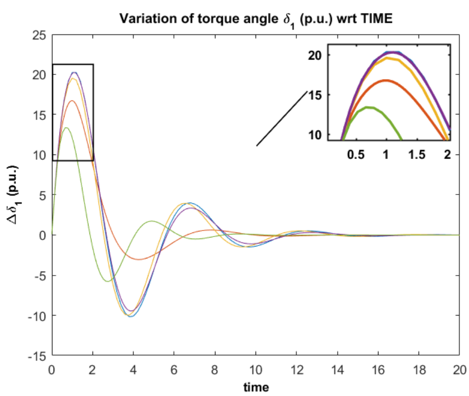

(e)

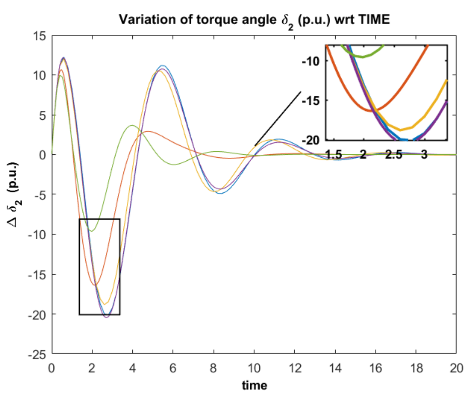

(f)

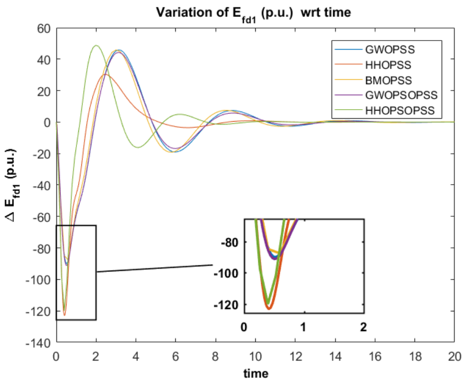

(g)

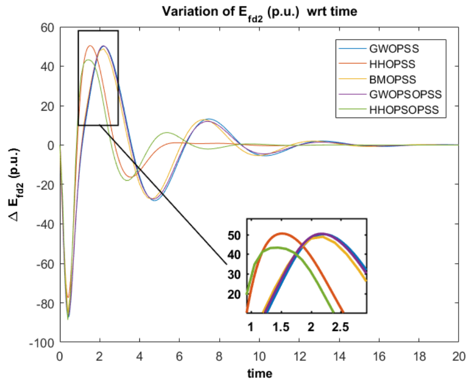

(h)

Figure 5: Damping behavior of system states for 10% perturbation under light load: (a) Angular speed of machine 1, (b) Angular speed of machine 2, (c) Generator 1 internal voltage, (d) Generator 2 internal voltage, (e) torque angle of area 1, (f) torque angle of area 2, (g) generator 1 field excitation voltage, (h) generator 2 field excitation voltage

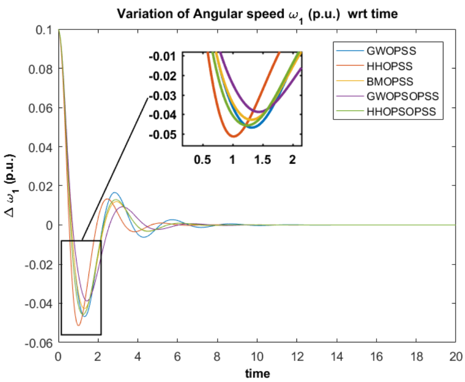

(a)

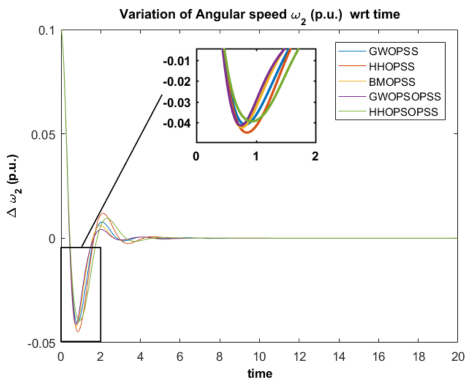

(b)

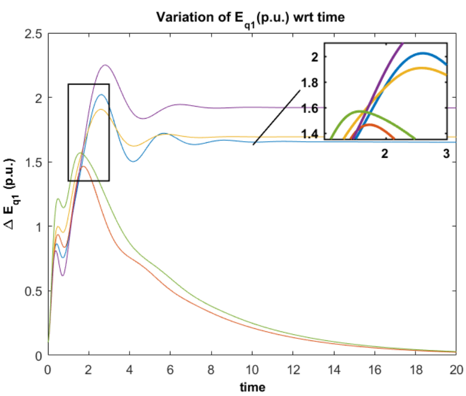

(c)

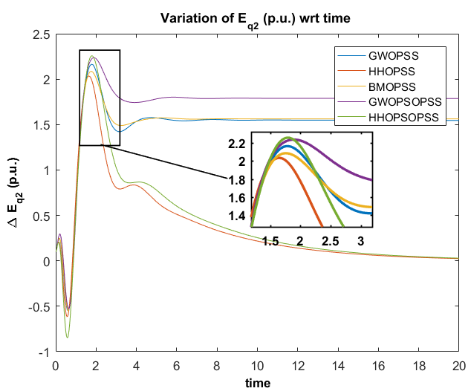

(d)

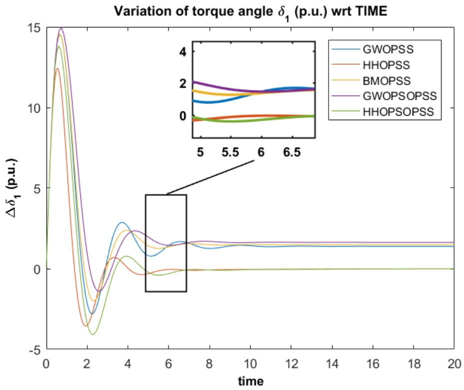

(e)

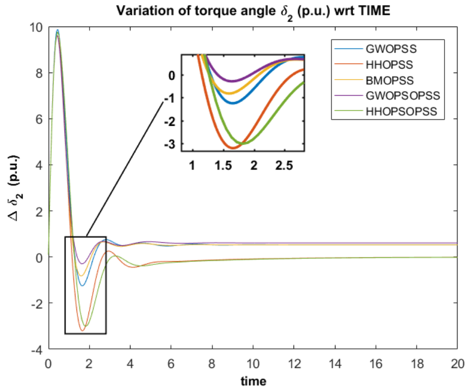

(f)

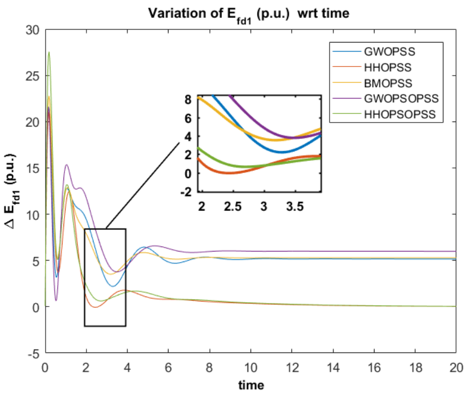

(g)

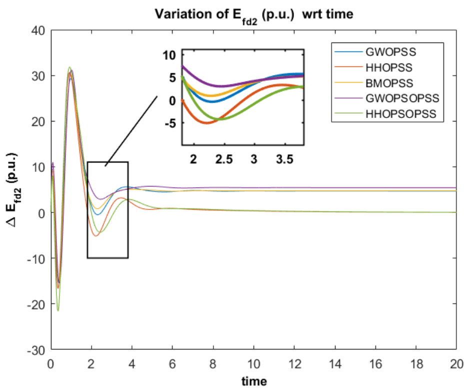

(h)

Figure 6: Damping behavior of system states for 10% perturbation under Nominal load: (a) Angular speed of machine 1, (b) Angular speed of machine 2, (c) Generator 1 internal voltage, (d) Generator 2 internal voltage, (e) torque angle of area 1, (f) torque angle of area 2, (g) generator 1 field excitation voltage, (h) generator 2 field excitation voltage

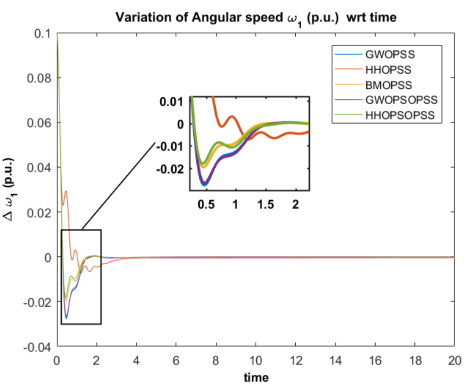

(a)

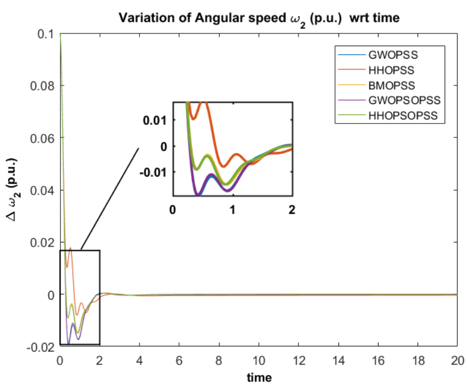

(b)

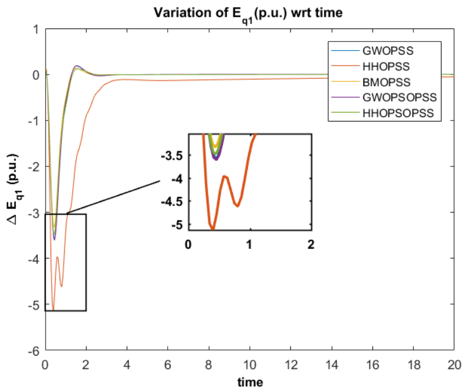

(c)

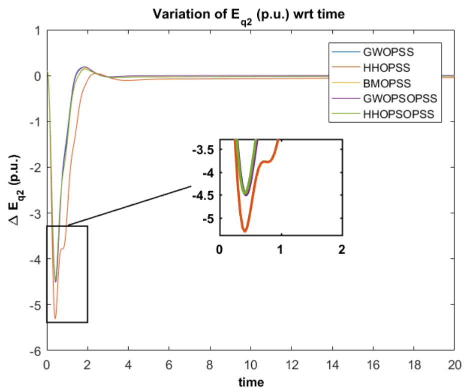

(d)

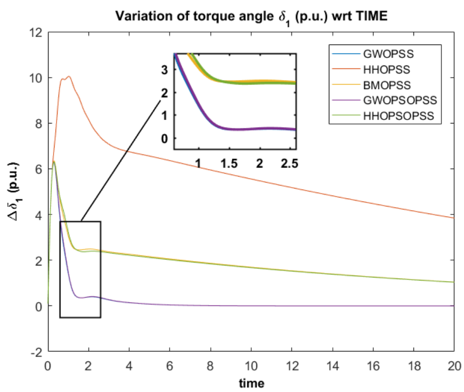

(e)

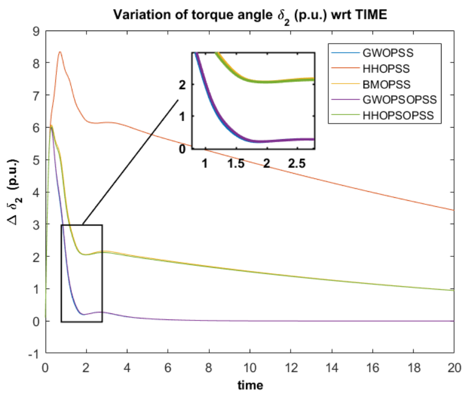

(f)

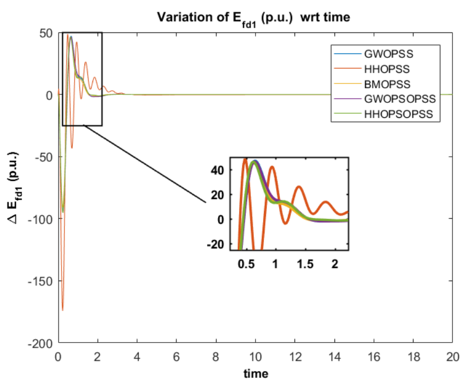

(g)

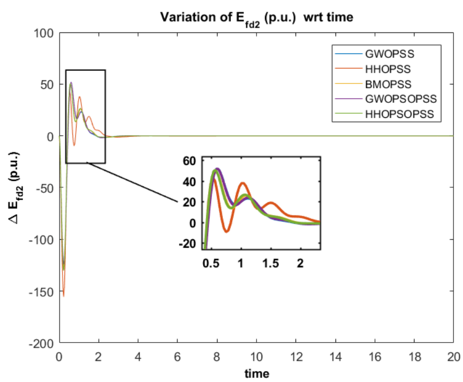

(h)

Figure 7: Damping behavior of system states for 10% perturbation under heavy load: (a) Angular speed of machine 1, (b) Angular speed of machine 2, (c) Generator 1 internal voltage, (d) Generator 2 internal voltage, (e) torque angle of area 1, (f) torque angle of area 2, (g) generator 1 field excitation voltage, (h) generator 2 field excitation voltage

for heavy loading condition is shown in Fig. 7. The performance of IHHO-PSO is next to GWO-PSO in terms of deviation in torque angle, but still its far better than HHO, which leads to an unstable mode of operation. For angular speed deviation BMO and proposed IHHO-PSO gives satisfactory results with minimum oscillation and fast operation. IHHO-PSO again proves its superiority over other algorithms like BMO, GWO-PSO etc.as it gives the smallest oscillation and zero deviation in the minimum time. The convergence characteristics suggest that IHHO-PSO can be efficiently used for tuning the system control parameters for the coordination of STATCOM with PSS.

6. Conclusion

The application of the proposed Integrated HHO-PSO algorithm in the engineering problem has shown superior performance over the state-of-the-art algorithms. The evaluation of the proposed algorithm on the benchmark functions justified the enhancements adopted for the HHO algorithm. The convergence of the IHHOPSO algorithm is better compared to the other trending algorithms and the considered hybrid algorithms. This paper presents a rigorous analysis of power system oscillations damping by the coordinated design of STATCOM and PSSs using meta-heuristic optimization algorithms. A two-area system with STATCOM connected in the middle of the transmission line has been modelled to perform the analysis on damping characteristics achieved with the proposed methods. For the selection of the appropriate tuning method from the proposed metaheuristic algorithms, the system study has been performed under different system loading conditions. The various analyses are performed based on the proposed technique convergence characteristics, the execution time for the considered system and the tuned parameters within the limits of the constraints. The system performances are analyzed through system eigenvalue location, damping ratios and damping nature offered to the system perturbations. By considering all the system analysis, the proposed IHHO-PSO tuned PSS parameters have been shown satisfactory performance characteristics and suggested over other proposed techniques for various system operating conditions.

References

[1] M. Črepinšek, S.-H. Liu, and L. Mernik: A note on teaching–learning-based optimization algorithm. *Information Sciences*, **212** (2012), 79–93, DOI: 10.1016/j.ins.2012.05.009.

[2] ANITA and A. YADAV: AEFA: Artificial electric field algorithm for global optimization. *Swarm and Evolutionary Computation*, **48** (2019), 93–108, DOI: 10.1016/j.swevo.2019.03.013.

[3] R. DEVARAPALLI and B. BHATTACHARYYA: A hybrid modified grey wolf optimization-sine cosine algorithm-based power system stabilizer parameter tuning in a multimachine power system. *Optimal Control Applications and Methods*, **41**(4), (2020), 1143-1159, DOI: 10.1002/oca.2591.

[4] M. JAIN, V. SINGH, and A. RANI: A novel nature-inspired algorithm for optimization: Squirrel search algorithm, *Swarm and Evolutionary Computation*, **44** (2019), 148–175, DOI: 10.1016/j.swevo.2018.02.013.

[5] A.E. EIBEN and J.E. SMITH: What is an Evolutionary Algorithm? In *Introduction to Evolutionary Computing*, Berlin, Heidelberg: Springer Berlin Heidelberg, 2015, 25–48, DOI: 10.1007/978-3-662-44874-8_3.

[6] A. KAVEH and M. KHAYATAZAD: A new meta-heuristic method: Ray Optimization. *Computers & Structures*, **112–113**, (2012), 283–294, DOI: 10.1016/j.compstruc.2012.09.003.

[7] P.J.M. VAN LAARHOVEN and E.H.L. AARTS: Simulated annealing. In *Simulated Annealing: Theory and Applications*, P.J.M. van Laarhoven and E.H.L. Aarts, Eds. Dordrecht: Springer Netherlands, 1987, 7–15, DOI: 10.1007/978-94-015-7744-1_2.

[8] A genetic algorithm tutorial. SpringerLink. https://link.springer.com/article/10.1007/BF00175354 (accessed Mar. 20, 2020).

[9] J. KENNEDY and R. EBERHART: Particle Swarm Optimization. *Proc. of ICNN'95 International Conference on Neural Networks*, **4** (1995), 1942–1948.

[10] M. NESHAT, G. SEPIDNAM, M. SARGOLZAEI, and A.N. TOOSI: Artificial fish swarm algorithm: a survey of the state-of-the-art, hybridization, combinatorial and indicative applications. *Artificial Intelligence Review*, **42**(4), (2014), 965–997, DOI: 10.1007/s10462-012-9342-2.

[11] M. DORIGO, M. BIRATTARI, and T. STUTZLE: Ant colony optimization. *IEEE Computational Intelligence Magazine*, **1**(4), (2006), 28–39, DOI: 10.1109/MCI.2006.329691.

[12] M. ROTH and S. WICKER: Termite: ad-hoc networking with stigmergy. In *GLOBECOM'03. IEEE Global Telecommunications Conference (IEEE Cat. No.03CH37489)*, **5** (2003), 2937–2941, DOI: 10.1109/GLOCOM.2003.1258772.

[13] D. Karaboga and B. Akay: A comparative study of Artificial Bee Colony algorithm. *Applied Mathematics and Computation*, **214**(1), (2009), 108–132, DOI: 10.1016/j.amc.2009.03.090.

[14] A. Mucherino and O. Seref: Monkey search: a novel metaheuristic search for global optimization. *AIP Conference Proceedings*, **953**(1), (2007), 162–173, DOI: 10.1063/1.2817338.

[15] E. Atashpaz-Gargari and C. Lucas: Imperialist competitive algorithm: An algorithm for optimization inspired by imperialistic competition. In *2007 IEEE Congress on Evolutionary Computation*, (2007), 4661–4667, DOI: 10.1109/CEC.2007.4425083.

[16] D. Simon: Biogeography-based optimization. *IEEE Transactions on Evolutionary Computation*, **12**(6), (2008), 702–713, DOI: 10.1109/TEVC.2008.919004.

[17] X.-S. Yang: Firefly algorithm. Stochastic, test, functions and design optimisation. *arXiv:1003.1409 [math]*, Mar. 2010, Accessed: Mar. 20, 2020. [Online]. Available: http://arxiv.org/abs/1003.1409.

[18] K.M. Gates and P.C.M. Molenaar: Group search algorithm recovers effective connectivity maps for individuals in homogeneous and heterogeneous samples. *NeuroImage*, **63**(1), (2012), 310–319, DOI: 10.1016/j.neuroimage.2012.06.026.

[19] E. Rashedi, H. Nezamabadi-Pour, and S. Saryazdi: GSA: A gravitational search algorithm. *Information Sciences*, **179**(13), (2009), 2232–2248, DOI: 10.1016/j.ins.2009.03.004.

[20] Y. Tan and Y. Zhu: Fireworks Algorithm for Optimization. In: Tan Y., Shi Y., Tan K.C. (eds) *Advances in Swarm Intelligence. ICSI 2010*. Lecture Notes in Computer Science, **6145**, Springer, Berlin, Heidelberg. DOI: 10.1007/978-3-642-13495-1_44.

[21] X.-S. Yang: Bat algorithm for multi-objective optimisation. *arXiv: 1203.6571 [math]*, Mar. 2012, Accessed: Mar. 20, 2020. [Online]. Available: http://arxiv.org/abs/1203.6571.

[22] Ling Wang, Xiao-long Zheng, and Sheng-yao Wang: A novel binary fruit fly optimization algorithm for solving the multidimensional knapsack problem. *Knowledge-Based Systems*, **48** 17–23, (2013), DOI: 10.1016/j.knosys.2013.04.003.

[23] X.-S. Yang: Flower Pollination Algorithm for Global Optimization. In *Unconventional Computation and Natural Computation*, Berlin, Heidelberg, 2012, 240–249, DOI: 10.1007/978-3-642-32894-7_27.

[24] G.-G. Wang, L. Guo, A.H. Gandomi, G.-S. Hao, and H. Wang: Chaotic Krill Herd algorithm. *Information Sciences*, **274** (2014), 17–34, DOI: 10.1016/j.ins.2014.02.123.

[25] A. Kaveh and N. Farhoudi: A new optimization method: Dolphin echolocation. *Advances in Engineering Software*, **59** (2013), 53–70, DOI: 10.1016/j.advengsoft.2013.03.004.

[26] S. Mirjalili, S.M. Mirjalili, and A. Lewis: Grey Wolf optimizer. *Advances in Engineering Software*, **69** (2014), 46–61, DOI: 10.1016/j.advengsoft.2013.12.007.

[27] A. Hatamlou: Black hole: A new heuristic optimization approach for data clustering. *Information Sciences*, **222** (2013), 175–184, DOI: 10.1016/j.ins.2012.08.023.

[28] A. Sadollah, A. Bahreininejad, H. Eskandar and M. Hamdi: Mine blast algorithm: A new population based algorithm for solving constrained engineering optimization problem. *Applied Soft Computing*, **13**(5), (2013), 2592–2612, DOI: 10.1016/j.asoc.2012.11.026.

[29] S. Mirjalili: Dragonfly algorithm: a new meta-heuristic optimization technique for solving single-objective, discrete, and multi-objective problems. *Neural Computing and Applications*, **27**(4), (2016), 1053–1073, DOI: 10.1007/s00521-015-1920-1.

[30] S. Mirjalili: Moth-flame optimization algorithm: A novel nature-inspired heuristic paradigm. *Knowledge-Based Systems*, **89** (2015), 228–249, DOI: 10.1016/j.knosys.2015.07.006.

[31] F.A. Hashim, E.H. Houssein, M.S. Mabrouk, W. Al-Atabany, and S. Mirjalili: Henry gas solubility optimization: A novel physics-based algorithm. *Future Generation Computer Systems*, **101** (2019), 646–667, DOI: 10.1016/j.future.2019.07.015.

[32] S. Mirjalili: The ant lion optimizer. *Advances in Engineering Software*, **83** (2015), 80–98, DOI: 10.1016/j.advengsoft.2015.01.010.

[33] H. Shareef, A.A. Ibrahim, and A.H. Mutlag: Lightning search algorithm. *Applied Soft Computing*, **36** (2015), 315–333, DOI: 10.1016/j.asoc.2015.07.028.

[34] S.A. Uymaz, G. Tezel, and E. Yel: Artificial algae algorithm (AAA) for nonlinear global optimization. *Applied Soft Computing*, **31** (2015), 153–171, DOI: 10.1016/j.asoc.2015.03.003.

[35] M.D. Li, H. Zhao, X.W. Weng, and T. Han: A novel nature-inspired algorithm for optimization: Virus colony search. *Advances in Engineering Software*, **92** (2016), 65–88, DOI: 10.1016/j.advengsoft.2015.11.004.

[36] O. Abedinia, N. Amjady, and A. Ghasemi: A new metaheuristic algorithm based on shark smell optimization. *Complexity*, **21**(5), (2016), 97–116, DOI: 10.1002/cplx.21634.

[37] S. Mirjalili, S.M. Mirjalili, and A. Hatamlou: Multi-Verse optimizer: a nature-inspired algorithm for global optimization. *Neural Computing and Applications*, **27**(2), (2016), 495–513, DOI: 10.1007/s00521-015-1870-7.

[38] S. Mirjalili and A. Lewis: The whale optimization algorithm. *Advances in Engineering Software*, **95** (2016), 51–67, DOI: 10.1016/j.advengsoft.2016.01.008.

[39] A. Askarzadeh: A novel metaheuristic method for solving constrained engineering optimization problems: Crow search algorithm. *Computers and Structures*, **169** (2016), 1–12, DOI: 10.1016/j.compstruc.2016.03.001.

[40] T. Wu, M. Yao, and J. Yang: Dolphin swarm algorithm. *Frontiers of Information Technology & Electronic Engineering*, **17**(8), (2016), 717–729, DOI: 10.1631/FITEE.1500287.

[41] S. Mirjalili: SCA: A sine cosine algorithm for solving optimization problems. *Knowledge-Based Systems*, **96** (2016), 120–133, DOI: 10.1016/j.knosys.2015.12.022.

[42] A. Kaveh and A. Dadras: A novel meta-heuristic optimization algorithm: Thermal exchange optimization. *Advances in Engineering Software*, **110**, (2017), 69–84, DOI: 10.1016/j.advengsoft.2017.03.014.

[43] M.M. Mafarja, I. Aljarah, A. Asghar Heidari, A.I. Hammouri, H. Faris, Ala'M. Al-Zoubi, and S. Mirjalili: Evolutionary population dynamics and grasshopper optimization approaches for feature selection problems. *Knowledge-Based Systems*, **145** (2018), 25–45, DOI: 10.1016/j.knosys.2017.12.037.

[44] A. tabari and A. Ahmad: A new optimization method: Electro-search algorithm. *Computers and Chemical Engineering*, **103** (2017), 1–11, DOI: 10.1016/j.compchemeng.2017.01.046.

[45] G. Dhiman and V. Kumar: Spotted hyena optimizer: A novel bio-inspired based metaheuristic technique for engineering applications. *Advances in Engineering Software*, **114** (2017), 48–70, DOI: 10.1016/j.advengsoft.2017.05.014.

[46] S.-A. Ahmadi: Human behavior-based optimization: a novel metaheuristic approach to solve complex optimization problems. *Neural Comput and Applications*, **28**(S1), (2017), 233–244, DOI: 10.1007/s00521-016-2334-4.

[47] A.F. Nematollahi, A. Rahiminejad, and B. Vahidi: A novel physical based meta-heuristic optimization method known as lightning attachment procedure optimization. *Applied Soft Computing*, **59** (2017), 596–621, DOI: 10.1016/j.asoc.2017.06.033.

[48] R.A. Ibrahim, A.A. Ewees, D. Oliva, M. Abd Elaziz, and S. Lu: Improved salp swarm algorithm based on particle swarm optimization for feature selection. *Journal of Ambient Intelligence and Humanized Computing*, **10**(8), (2019), 3155–3169, DOI: 10.1007/s12652-018-1031-9.

[49] E. Jahani and M. Chizari: Tackling global optimization problems with a novel algorithm – Mouth brooding fish algorithm. *Applied Soft Computing*, **62** (2018), 987–1002, DOI: 10.1016/j.asoc.2017.09.035.

[50] X. Qi, Y. Zhu, and H. Zhang: A new meta-heuristic butterfly-inspired algorithm. *Journal of Computational Science*, **23** (2017), 226–239, DOI: 10.1016/j.jocs.2017.06.003.

[51] S. Mirjalili: Moth-flame optimization algorithm: A novel nature-inspired heuristic paradigm. *Knowledge-Based Systems*, **89** (2015), 228–249, DOI: 10.1016/j.knosys.2015.07.006.

[52] M. Dorigo, V. Maniezzo, and A. Colorni: Ant system: optimization by a colony of cooperating agents. *IEEE Transactions on Systems, Man, and Cybernetics, Part B (Cybernetics)*, **26**(1), (1996), 29–41, DOI: 10.1109/3477.484436.

[53] S. Mirjalili and S.Z.M. Hashim: A new hybrid PSOGSA algorithm for function optimization. In *2010 International Conference on Computer and Information Application*, (2010), 374–377, DOI: 10.1109/ICCIA.2010.6141614.

[54] F.A. Şenel, F. Gökçe, A.S. Yüksel, and T. Yiğit: A novel hybrid PSO–GWO algorithm for optimization problems. *Engineering with Computers*, **35**(4), 1359–1373, DOI: 10.1007/s00366-018-0668-5.

[55] D.T. Bui, H. Moayedi, B. Kalantar, and A. Osouli: Harris hawks optimization: A novel swarm intelligence technique for spatial assessment of landslide susceptibility. *Sensors*, **19**(14), (2019), 3590, DOI: 10.3390/s19163590.

[56] H. Chen, S. Jiao, M. Wang, A.A. Heidari, and X. Zhao: Parameters identification of photovoltaic cells and modules using diversification-enriched Harris hawks optimization with chaotic drifts. *Journal of Cleaner Production*, **244** (2020), p. 118778, DOI: 10.1016/j.jclepro.2019.118778.

[57] A.A. Heidari, S. Mirjalili, H. Faris, I. Aljarah, M. Mafarja, and H. Chen: Harris hawks optimization: Algorithm and applications. *Future Generation Computer Systems*, **97** (2019), 849–872, DOI: 10.1016/j.future.2019.02.028.

[58] M. Jamil and X.-S. Yang: A literature survey of benchmark functions for global optimization problems. *International Journal of Mathematical Modelling and Numerical Optimisation*, **4**(2), (2013), 150, DOI: 10.1504/IJMMNO.2013.055204.

[59] A. Kaveh and S. Talatahari: A novel heuristic optimization method: charged system search. *Acta Mechanica*, **213**(3–4), (2010), 267–289, DOI: 10.1007/s00707-009-0270-4.

[60] J. Luo and B. Shi: A hybrid whale optimization algorithm based on modified differential evolution for global optimization problems. *Applied Intelligence*, **49**(5), (2000), 1982–2000, DOI: 10.1007/s10489-018-1362-4.

[61] A.A. Heidari, S. Mirjalili, H. Faris, I. Aljarah, M. Mafarja, and H. Chen: Harris hawks optimization: Algorithm and applications. *Future Generation Computer Systems*, **97** (2019), 849–872, DOI: 10.1016/j.future.2019.02.028.

[62] P. Pruski and S. Paszek: Location of generating units most affecting the angular stability of the power system based on the analysis of instantaneous power waveforms. *Archives of Control Sciences*, **30**(2), (2020), 273–293, DOI: 10.24425/acs.2020.133500.

[63] M.M. Hossain and A.Z. Khurshudyan: Heuristic control of nonlinear power systems: Application to the infinite bus problem. *Archives of Control Sciences*, **29**(2), (2019), 279–288, DOI: 10.24425/acs.2019.129382.

[64] R. Devarapalli and B. Bhattacharyya: A framework for $H_2/H_?$ synthesis in damping power network oscillations with STATCOM. *Iranian Journal of Science and Technology, Transactions of Electrical Engineering*, **44** (2020), 927-948, DOI: 10.1007/s40998-019-00278-4.

[65] G. Gurrala and I. Sen: Power system stabilizers design for interconnected power systems. *IEEE Transactions on Power Systems*, **25**(2), (2010), 1042–1051, DOI: 10.1109/TPWRS.2009.2036778.

[66] R.K. Varma: Introduction to FACTS controllers. In *2009 IEEE/PES Power Systems Conference and Exposition*, (2009), 1–6, DOI: 10.1109/PSCE.2009.4840114.

[67] P. Kundur: *Power System Stability and Control*. Tata McGraw-Hill Education, 1994.

[68] M. Belazzoug, M. Boudour, and K. Sebaa: FACTS location and size for reactive power system compensation through the multi-objective optimization. *Archives of Control Sciences*, **20**(4), (2010), 473–489, DOI: 10.2478/v10170-010-0027-2.